

Chulalongkorn University

Chula Digital Collections

Chulalongkorn University Theses and Dissertations (Chula ETD)

2022

Production of PD-L1 immune checkpoint inhibitor in nicotiana benthamiana

Thareeya Phetphoung

Faculty of Pharmaceutical Sciences

Follow this and additional works at: <https://digital.car.chula.ac.th/chulaetd>

Recommended Citation

Phetphoung, Thareeya, "Production of PD-L1 immune checkpoint inhibitor in nicotiana benthamiana" (2022). *Chulalongkorn University Theses and Dissertations (Chula ETD)*. 6008.
<https://digital.car.chula.ac.th/chulaetd/6008>

This Thesis is brought to you for free and open access by Chula Digital Collections. It has been accepted for inclusion in Chulalongkorn University Theses and Dissertations (Chula ETD) by an authorized administrator of Chula Digital Collections. For more information, please contact ChulaDC@car.chula.ac.th.

PRODUCTION OF PD-L1 IMMUNE CHECKPOINT INHIBITOR IN *NICOTIANA BENTHAMIANA*



A Thesis Submitted in Partial Fulfillment of the Requirements
for the Degree of Master of Science in Pharmaceutical Sciences and Technology
FACULTY OF PHARMACEUTICAL SCIENCES
Chulalongkorn University
Academic Year 2022
Copyright of Chulalongkorn University

การผลิตด้วยปั๊มจุดตรวจภูมิคุ้มกันพีดีแอลวันในต้นยาสูบ



วิทยานิพนธ์นี้เป็นส่วนหนึ่งของการศึกษาตามหลักสูตรปริญญาวิทยาศาสตรมหาบัณฑิต

สาขาวิชาเภสัชศาสตร์และเทคโนโลยี ไม่สังกัดภาควิชา/เทียบเท่า

คณะเภสัชศาสตร์ จุฬาลงกรณ์มหาวิทยาลัย

ปีการศึกษา 2565

ลิขสิทธิ์ของจุฬาลงกรณ์มหาวิทยาลัย

Thesis Title	PRODUCTION OF PD-L1 IMMUNE CHECKPOINT INHIBITOR IN <i>NICOTIANA BENTHAMIANA</i>
By	Miss Thareeya Phetphoung
Field of Study	Pharmaceutical Sciences and Technology
Thesis Advisor	Associate Professor WARANYOO PHOOLCHAROEN, Ph.D.

Accepted by the FACULTY OF PHARMACEUTICAL SCIENCES, Chulalongkorn
University in Partial Fulfillment of the Requirement for the Master of Science

..... Dean of the FACULTY OF
PHARMACEUTICAL SCIENCES
(Professor PORNANONG ARAMWIT, Ph.D.)

THESIS COMMITTEE

..... Chairman
(Associate Professor SORNKANOK VIMOLMANGKANG,
Ph.D.)

..... Thesis Advisor
(Associate Professor WARANYOO PHOOLCHAROEN, Ph.D.)

..... Examiner
(Assistant Professor SUPANNIKAR TAWINWUNG, Ph.D.)

..... Examiner
(Associate Professor Chatchai Chaotham, Ph.D.)

..... External Examiner
(Assistant Professor Kittipong Rattanaorn, Ph.D.)

ธารีญา เพ็ชรผึ้ง : การผลิตด้วยยั้งจุดตรวจภูมิคุ้มกันพีดีแอลวันในต้นยาสูบ. (PRODUCTION OF PD-L1 IMMUNE CHECKPOINT INHIBITOR IN *NICOTIANA BENTHAMIANA*) อ.ที่ปรึกษาหลัก : รศ. ดร.วรัญญู พูลเจริญ

แอนติบอดีที่ขัดขวางการจับกันระหว่างตัวรับและลิแกนด์ของจุดตรวจภูมิคุ้มกันได้ถูกศึกษาสำหรับการรักษาโรคมะเร็งโดยจะไปรบกวนการทำงานที่ในการควบคุมสมดุลของระบบภูมิคุ้มกัน การออกแบบแอนติบอดีเพื่อยับยั้งการจับกันระหว่างพีดีวันและพีดีแอลวันเป็นเป้าหมายสำคัญหนึ่งที่ใช้ในวิธีการรักษามะเร็งด้วยภูมิคุ้มกันบำบัด อะทีโซลิซูแมบ (Atezolizumab) เป็นแอนติบอดีตัวแรกที่มุ่งเป้าไปยังพีดีแอลวันลิแกนด์ มีศักยภาพและได้รับการอนุมัติในการรักษามะเร็งระยะแพร่กระจายหลายชนิด อันได้แก่ มะเร็งท่อน้ำนม มะเร็งปอดชนิดเซลล์เล็ก มะเร็งปอดชนิดเซลล์ไม่เล็ก และมะเร็งเต้านมชนิดที่ไม่แสดงตัวรับทั้งสามชนิด อย่างไรก็ตามกระบวนการผลิตอะทีโซลิซูแมบที่ใช้เซลล์สัตว์เลี้ยงลูกด้วยนม ซึ่งคือ Chinese Hamster Ovary เป็นระบบที่มีต้นทุนในการผลิตสูง ศักยภาพในการผลิตต่ำ และมีความเสี่ยงต่อการปนเปื้อนได้ง่าย งานวิจัยนี้จึงมีวัตถุประสงค์เพื่อทำการศึกษาการผลิตแอนติบอดีในใบยาสูบ (*Nicotiana benthamiana*) ด้วยวิธีการแสดงออกแบบชั่วคราวที่มีความสามารถในการผลิตได้อย่างรวดเร็ว ได้ผลผลิตปริมาณมาก และมีต้นทุนต่ำ โดยการนำเชื้อ *Agrobacterium tumefaciens* GV3101 ที่มียีนของอะทีโซลิซูแมบในพลาสมิดนำเข้าสู่ใบยาสูบ พบว่า การผลิตด้วยกระบวนการนี้ใบยาสูบมีการแสดงออกอะทีโซลิซูแมบ 86.76 ไมโครกรัมต่อกรัมของน้ำหนักใบไม้สด เมื่อฉีดเชื้อแบคทีเรียที่มีความเข้มข้น $OD_{600} = 0.4$ เก็บใบไม้ในวันที่ 6 หลังการฉีดเชื้อ และใช้เชื้อที่มียีนส่วนเส้นหนักต่อเส้นเบาเท่ากับ 1:1 นอกจากนี้ ผลการทดสอบสมบัติทางโครงสร้างและหน้าที่ของพีดีแอลวันแอนติบอดีที่ผลิตจากพืชเปรียบเทียบกับยาต้นแบบ Tecentriq® ที่ผลิตจาก Chinese Hamster Ovary พบว่ามีความสามารถในการจับกับตัวรับพีดีแอลวันได้คล้ายคลึงกัน ดังนั้น จากงานวิจัยนี้พบว่าต้นยาสูบสามารถนำมาใช้เป็นทางเลือกในการผลิตที่มีความคุ้มค่าต่อต้นทุนประสิทธิผล โดยผู้วิจัยคาดหวังว่าจะสามารถพัฒนากระบวนการนี้เพื่อใช้ผลิตแอนติบอดีที่มีศักยภาพเพียงพอในการใช้รักษามะเร็งได้

สาขาวิชา เกษษศาสตร์และเทคโนโลยี ลายมือชื่อนิสิต

ปีการศึกษา 2565 ลายมือชื่อ อ.ที่ปรึกษาหลัก

6470006033 : MAJOR PHARMACEUTICAL SCIENCES AND TECHNOLOGY

KEYWORD: Anti-PD-L1, Atezolizumab, Cancer immunotherapy, *Nicotiana benthamiana*, Transient expression

Thareeya Phetphoung : PRODUCTION OF PD-L1 IMMUNE CHECKPOINT INHIBITOR IN *NICOTIANA BENTHAMIANA*. Advisor: Assoc. Prof. WARANYOO PHOOLCHAROEN, Ph.D.

Immune checkpoint antibodies disrupt the binding of receptor-ligand pairs which regulate immune response in cancer treatment. PD-1/PD-L1 pathway has become one target of the cancer immunotherapy approaches. Atezolizumab, the first FDA-approved antibody to PD-L1 in the treatment of metastatic urothelial, non-small cell lung, small cell lung, and hepatocellular cancers, is expressed in Chinese Hamster Ovary (CHO) cell lines with several limitations, *i.e.*, high costs of production, limited-capacity yields, and pathogen risks. To overcome these drawbacks, the transient expression in *Nicotiana benthamiana* leaves, which provide expandable scalability and inexpensive costs, was investigated by co-infiltration of *Agrobacterium tumefaciens* GV3101 cultures harboring Atezolizumab heavy chain and light chain in the genes of interest sites. The transient expression of Atezolizumab produced up to 86.76 micrograms/gram of fresh leaf weight after agroinfiltrated with OD 600 nm = 0.4 and 1:1 heavy chain to light chain ratio, then harvested on 6 days post-infiltration. The plant-produced anti-PD-L1 was assessed for physicochemical and functional properties compared to commercially available Tecentriq® from CHO cells, which showed similar binding efficacies to PD-L1 receptors. In conclusion, this research provides plants with an alternative cost-effective platform for producing functional monoclonal antibodies for cancer therapy.

Field of Study: Pharmaceutical Sciences Student's Signature
and Technology

Academic Year: 2022 Advisor's Signature

ACKNOWLEDGEMENTS

Foremost, these words still cannot express all of my gratitude through the two years of my master's degree; however, I would like to acknowledge all people and all institutes for being part of my success.

The first and most important thanks are given to my thesis advisor, Associate Professor Waranyoo Phoolcharoen, Ph.D. from the Department of Pharmacognosy and Pharmaceutical Botany, Faculty of Pharmaceutical Sciences, Chulalongkorn University, for all opportunities, valuable guidance, and continuous support. I would like to extend thanks to Associate Professor Chatchai Chaotham, Ph.D., who became my publication advisor, for his encouragement and assistance. However, I still would like to express this gratitude to Associate Professor Richard Stasser, Ph.D., for warm-welcoming and unforgettable experiences in Vienna. In addition, I have to thank labmates and researchers in the WP lab for your help, your support, and our friendship.

Besides, my long journey cannot be accomplished without the financial support from Chulalongkorn University Graduate School for Chulalongkorn University Graduate Scholarship to commemorate the 72nd Anniversary of His Majesty King Bhumibol Adulyadej, the 90th Anniversary of Chulalongkorn University Fund (Ratchadaphiseksomphot Endowment Fund) and the Overseas Research Experience Scholarship. Also, I would like to thank the Pharmaceutical Sciences and Technology (PST) program, Faculty of Pharmaceutical Sciences, Chulalongkorn University.

Last but not least, I would like to give the deepest thanks to myself, my family, and my friends for always being supportive with love and understanding.

Thareeya Phetphoung

TABLE OF CONTENTS

	Page
ABSTRACT (THAI)	iii
ABSTRACT (ENGLISH)	iv
ACKNOWLEDGEMENTS	v
TABLE OF CONTENTS	vi
LIST OF TABLES	viii
LIST OF FIGURES	ix
CHAPTER I INTRODUCTION.....	1
1.1 Rationale and significant.....	1
1.2 Research hypotheses.....	3
CHAPTER II LITERATURE REVIEW	4
2.1 Cancer and cancer treatments.....	4
2.2 Cancer immunotherapy	6
2.3 Immune checkpoint.....	10
2.4 PD-1/PD-L1 checkpoint	11
2.5 Atezolizumab	13
2.6 Antibody.....	14
2.7 Molecular pharming in <i>Nicotiana benthamiana</i>	17
CHAPTER III MATERIALS AND METHODS	26
3.1 Materials and Equipment	26
3.2 Method.....	32
3.2.1 Construction of Recombinant Vector	32

3.2.1.1 Gene design and gene synthesis	32
3.2.1.2 Recombinant plasmid cloning	33
3.2.2 Transient Expression with Optimization Conditions of Anti-PD-L1 Antibody in <i>Nicotiana benthamiana</i>	36
3.2.3 Purification of Plant-produced Atezolizumab.....	37
3.2.4 Identification of Anti-PD-L1 Antibody with SDS-PAGE and Western Blotting	37
3.2.5 Quantification of Anti-PD-L1 Antibody Amount with Sandwich ELISA Technique	38
3.2.6 N-Glycan Analysis.....	39
3.2.7 Human PD-L1 Specific Binding Assay	39
3.2.8 PD-1/PD-L1 Blockade Bioassay.....	40
CHAPTER IV RESULTS	41
4.1 Optimization Conditions for Anti-PD-L1 Expression	41
4.2 Extraction and Purification of Anti-PD-L1 from <i>N. benthamiana</i>	42
4.3 N-Linked Glycosylation Pattern of Anti-PD-L1 Antibody	43
4.4 Functional Assays of Plant-produced Anti-PD-L1 Antibody	44
CHAPTER V DISCUSSION AND CONCLUSION	46
APPENDICES.....	50
APPENDIX A: Amino Acid and Nucleotide Sequences.....	51
APPENDIX B: Cloning and Expression Vectors	55
APPENDIX C: Chemical Solutions Preparation.....	57
REFERENCES	63
VITA.....	74

LIST OF TABLES

	Page
Table 1: Cancer therapy approaches and mechanism of action.	6
Table 2: FDA-approved immune checkpoint blockers.....	11
Table 3: Comparison of recombinant protein expression systems.	18
Table 4: Plant-based platforms for protein production.....	20
Table 5: Primers used in PCR for confirming the selected bacterial clones.....	35



LIST OF FIGURES

	Page
Figure 1: The six hallmarks of carcinogenesis.....	4
Figure 2: Distribution of cancer cases and deaths in 2020.	5
Figure 3: Interaction of immune co-stimulatory/co-inhibitory signals.....	7
Figure 4: Cancer immunotherapy agents.....	9
Figure 5: Signaling pathway involved with PD-1 and PD-L1 expression.....	12
Figure 6: Antibody structure.....	15
Figure 7: N-Glycosylation patterns in plants and animals.	17
Figure 8: Schematic of protein N-glycosylation pathways in plants.....	22
Figure 9: Schematic of plant glycosylation engineering strategies.....	22
Figure 10: Structure of tumor-inducing (Ti) plasmid found in <i>Agrobacterium tumefaciens</i>	23
Figure 11: The essential steps of <i>Agrobacterium tumefaciens</i> transformation.	24
Figure 12: The schematic diagram of light chain (A) and heavy chain (B) of anti-PD-L1 for construction design.....	33
Figure 13: The schematic diagram of T-DNA regions in geminiviral vector (pBYR2e) for the plant-produced anti-PD-L1 antibody expression.....	35
Figure 14: Pattern for agroinfiltration in optimization of antibody expression.....	36
Figure 15: Optimization conditions of optical density (OD) of <i>Agrobacterium tumefaciens</i> , days post-infiltration (dpi), and heavy chain to light chain ratio.	42
Figure 16: SDS-PAGE and Western blotting of purified anti-PD-L1 antibody under non-reducing and reducing conditions.....	43
Figure 17: Liquid chromatography-electrospray ionization-mass spectrometry (LC-ESI-MS) of Tecentriq® and plant-produced PD-L1 antibody after trypsin digestion.	44

Figure 18: Binding and inhibition assays of plant-produced anti-PD-L1 antibody. 45



CHAPTER I INTRODUCTION

1.1 Rationale and significant

Cancer is a common cause of mortality. Lung, breast, colorectum, and prostate cancers are the most frequently discovered cancers worldwide. Even though chemotherapy is commonly used for cancer therapy, they still have many drawbacks, such as severe adverse effects, expensive treatments, and overcoming therapeutic plateau. ⁽¹⁾ Nowadays, cancer immunotherapy has emerged as a favorable technology in the last few decades from the knowledge that tumors are precisely recognized and eliminated by the host immune system, leading to the discovery of effective and less toxic treatments. The Food and Drug Administration (FDA) has approved the various cancer immunotherapy approaches comprising cell therapy, cancer vaccines, immunomodulators, oncolytic virus, and immune checkpoint antibodies. ⁽²⁾ Normally, adaptive immune system produces tumor antigen-specific T-cells that can destroy cancer cells. Immune checkpoints (ICs), e.g., CTLA-4, PD-L1, PD-1, and others, are receptor-ligand pairs that effectively modulate cancer immunity. ⁽³⁻⁵⁾ However, cancerous cells also use the immune defense mechanism to escape from the host immune system. The PD-1/PD-L1 pathway has been a keen interest for use in cancer immunotherapy. The binding of the PD-1 receptor on T-cells to its ligands on cancer cells leads to T-cell deactivation and apoptosis. ^(6, 7)

FDA approved several immune checkpoint inhibitors which have shown outstanding clinical benefits in various tumor types. ⁽⁸⁾ The programmed cell death receptor ligand 1 or PD-L1, also known as B7-H1 or CD274, comprises of 290 amino acids, is the group of type I transmembrane protein receptors in the B7 family, and is commonly present on T-cells, B-cells, monocytes and antigen-presenting cells (APC's). The PD-1/PD-L1 checkpoint signaling is the critical pathway for the tumor

evasion from immune scrutiny.⁽⁹⁾ Hence, immune checkpoint blockers have gained major interest in recent times from different types of cancer patients with tumor cells or infiltrating immune cell populations expressing PD-L1 ligands.⁽¹⁰⁾ Atezolizumab is a highly specific humanized IgG1 antibody which can block the interaction of PD-L1 ligand expressed on tumor cells with the PD-1 receptors on the T-cell population, thereby reducing the immunosuppressive action of tumor-inducing cells and enhancing the adaptive immune responses in the host against tumors.⁽¹¹⁾ This FDA approved monoclonal antibody was used as the first-line drug in the treatment of metastatic non-small cell lung cancerous cells (NSCLC's) with moderate or high PD-L1 expression. The treatment with Atezolizumab has also shown significant increase in survival time periods when compared to chemotherapy. Furthermore, it can be used in combination with chemotherapy, cell therapy or other treatments to improve clinical responses.⁽¹²⁻¹⁴⁾

Atezolizumab, a humanized monoclonal non-glycosylated antibody, was produced in Chinese Hamster Ovary (CHO) cells.⁽¹⁵⁾ The production of recombinant complex proteins in mammalian cell lines has been proved as the potential expression system with several limitations, i.e., high-production costs, low capacity, and contamination risks.⁽¹⁶⁾ Alternatively, plant expression systems have gained major interest in making recombinant proteins due to the economical production costs in upstream processes, rapid scalability employing versatile growth conditions, and pathogen-free with low contamination risks.^(3, 17) *Nicotiana* genus has been widely used in establishing a history in the production of heterologous recombinant proteins that include antibodies⁽¹⁸⁻²⁰⁾, vaccines^(21, 22), enzymes^(23, 24), growth factors⁽²⁵⁻²⁷⁾, diagnostics⁽²⁸⁾, anti-microbial peptides⁽²⁹⁾ and other value-added products⁽³⁰⁾ because of the ease in genome manipulation and fast growth rate.^(31, 32) The transient expression by agroinfiltration was adopted in plants to produce various

proteins for therapeutic use. *Agrobacterium*-mediated gene transfer incorporates the gene of interest in the T-DNA region of the plant cell for protein expression.⁽³³⁾

Atezolizumab, the first line therapy approved globally for metastatic non-small cell lung cancer, involves high treatment costs. The current study aimed to use *N. benthamiana* as the host system for the transient expression of the variable region of Atezolizumab, an anti-human PD-L1 antibody. The plant-expressed anti-PD-L1 proteins were characterized for their physicochemical and functional attributes compared with the commercial Atezolizumab (Tecentriq®). The *in vitro* obtained results showed similar binding affinities to PD-L1 protein, stimulating immune responses. Hence, this study forms the proof of concept for using plant-produced monoclonal antibodies in cancer therapy.

1.2 Research hypotheses

1. The anti-PD-L1 antibody can be transiently produced in *Nicotiana benthamiana*.
2. The plant-produced anti-PD-L1 antibody shows the potential for use as cancer therapeutic when compared to Atezolizumab (Tecentriq®)

CHAPTER II LITERATURE REVIEW

2.1 Cancer and cancer treatments

Cancer refers to a group of various diseases involving abnormal cell growth. Normal cells are regulated with stimulatory and inhibitory signals. The cells are altered into cancer cells when the normal cells are damaged with carcinogens and then irregularly proliferate during cell division. Carcinogens include physical, chemical, and biological agents exposed to the cells, resulting in aberrant cell responses. However, genetic and epigenetic changes subsequently play an important role in carcinogenesis. The primary physical characteristics of cancer cell growth are shown in Figure 1. Tumor cells require multiple steps of alteration that develop into uncontrolled cell growth, tissue invasion, and metastases. ^(34, 35)

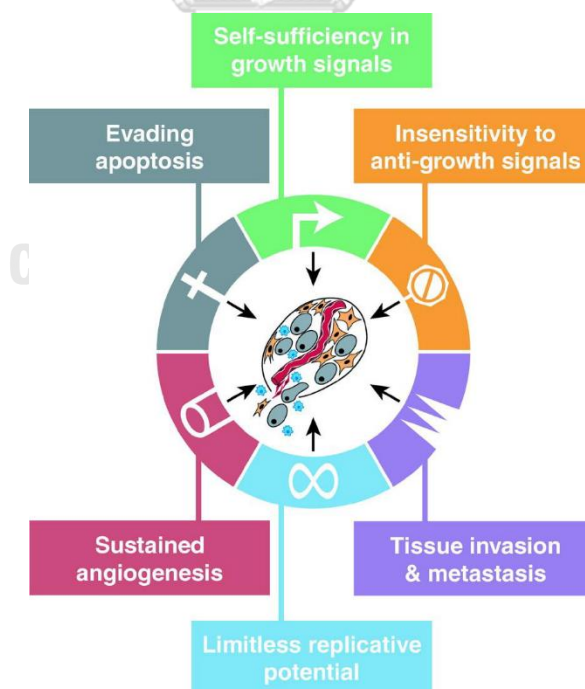


Figure 1: The six hallmarks of carcinogenesis. ⁽³⁵⁾

Cancer is a critical health disease and the leading cause of mortality worldwide. Cancer incidence has been increasing in this decade. In 2020, new cancer cases were diagnosed at 19.3 million, and the patient deaths are up to 9.9 million, presented in Figure 2. The most common cancer types are breast, lung, colorectal, and prostate cancer, respectively. ⁽³⁶⁾

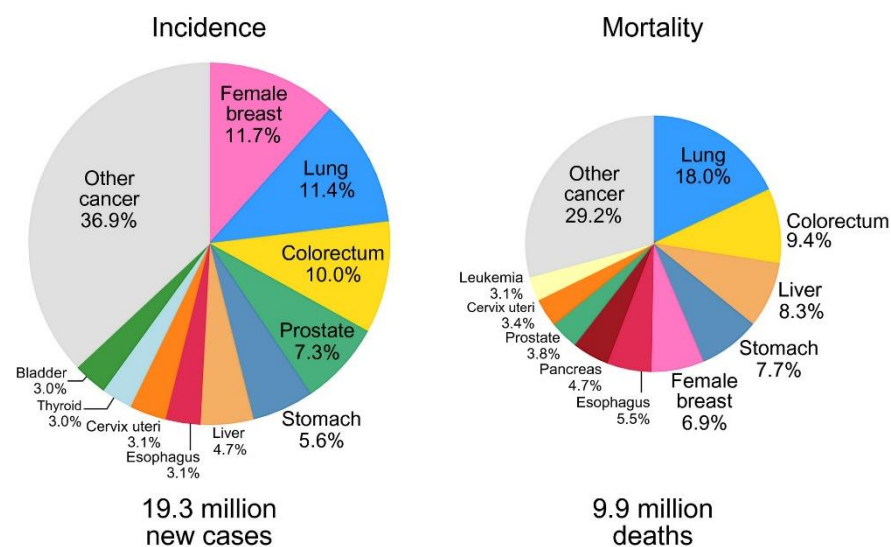


Figure 2: Distribution of cancer cases and deaths in 2020. ⁽³⁶⁾

Cancer treatments have been divided into localized treatments and systematic treatments. The ultimate goal of treatment is to remove cancer cells. However, the actual purpose of treating cancer patients depends on malignant types and their stages. Local cancer therapy is commonly surgery, radiation therapy, and other ablative approaches. Systematic treatments include chemotherapy agents, targeted molecular therapies, and cancer immunotherapies. Non-specific cytotoxic agents target DNA or microtubules in normal and cancer cells. ^(37, 38) Consequently, chemotherapy causes various side effects, such as alopecia, nausea, vomiting, fatigue, mouth sores, gastrointestinal problems, and mood disturbance. ⁽³⁹⁾ In achieving effective treatment, diverse approaches are combined to reduce adverse events and

increase efficacy. Targeted inhibitors are developed by focusing on individual targets expressed on tumors. Nevertheless, the inhibitors also fail to bind to their targets. Biological therapy is interested in cancer immunotherapy via activation of the host immune system to eradicate tumors specifically.^(38, 40) The summary of cancer treatments is briefly described in table 1.

Table 1: Cancer therapy approaches and mechanism of action.⁽⁴⁰⁾

Type of therapy	Mechanism of action
Chemotherapy	
Cytostatic drugs	Inhibit cell proliferation
Small molecule inhibitors (or targeted therapy) e.g., sunitinib, imatinib, sorafenib and lapatinib	Inhibit signal transduction
Biological cancer therapy	
Anti-tumor monoclonal antibodies e.g., cetuximab, trastuzumab, panitumumab	Targeted immunotherapy
Anti-angiogenesis monoclonal antibodies e.g., bevacizumab (VEGF-L), ramucirumab (VEGF receptor 2)	Inhibit angiogenesis
Checkpoint inhibitor monoclonal antibodies e.g., ipilimumab (CTLA-4), nivolumab (PD-1), atezolizumab, and durvalumab (PD-L1)	Immune regulation
CAR-T cells	Target to CD8+ T-cells
Anti-tumor vaccines	Active specific vaccination
Oncolytic viruses e.g., RNA viruses	Oncolysis

2.2 Cancer immunotherapy

Cancer immunotherapies are considered based on the knowledge of cancer physiology, cancer immunology, and host immune responses. The immune cells

typically recognize foreign antigens, both internal and external substances. The immune system can precisely bind to tumor-associated antigens (TAAs), and then cancerous cells are eliminated through the process called ‘immune surveillance’. However, the late-stage tumor has the ability to escape from adaptive immune attacks. These circumstances are considered a hallmark for generating anti-tumor agents by promoting antigen-presenting cells, activating T-cell responses, and inhibiting immunosuppression. ^(2, 41)

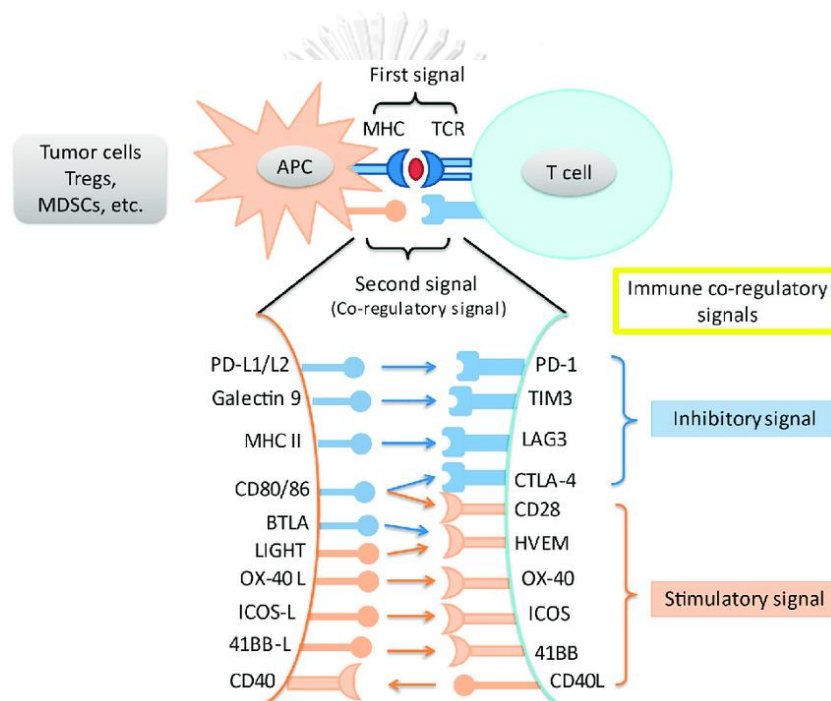


Figure 3: Interaction of immune co-stimulatory/co-inhibitory signals. ⁽⁴²⁾

Antigen-presenting cells, especially dendritic cells, will detect TAAs on tumor cells, process the antigens, and present them on MHC molecules. Following this, the dendritic cells migrate to lymphoid organs to present the antigens to CD4⁺ T-cells that are induced to Th1, Th2, and Treg cells. The stimulation of T-cells depends on co-stimulatory molecules bound with dendritic cells. T-cells promotion is activated through the interaction of CD28 and CD80/86, while T-cells suppression is controlled with the binding of CTLA4 and CD80/86 or PD-1 with PD-L1/PD-L2. The effective T-

cells can eliminate cancerous cells in the tumor bed, where cancer will upregulate PD-L1/L2 and release suppressors to defense T-cell responses. ⁽⁴¹⁾

Monoclonal Antibodies⁽²⁾

Monoclonal antibodies (mAbs) are used to treat various malignancy types, both lymphomas and solid tumors. The mAbs are artificially produced by specific B-cell clones that can bind to TAAs. Therapeutic mAbs include immunoglobulin G, antibody fragments, and conjugated mAbs. The common mechanisms of action of mAbs are relevant to antibody-dependent cellular cytotoxicity, complement-dependent cytotoxicity, cell death signaling, angiogenesis, and immune checkpoints. Moreover, the conjugation of mAbs with cytotoxic drugs, radionuclides, or polymers can increase the efficacy of cancer cell destruction.

Cytokines⁽²⁾

Cytokines are produced by the immune cells to control the balance of immunity and inflammation. Cytokines are small peptides that include chemokines, growth factors, interferons, interleukins, and lymphokines. Many cytokines are involved in cancer immunity by inducing or inhibiting T-cell responses. Nowadays, IFN- α and IL-2 have been approved for cancer immunotherapy.

Cancer Vaccines⁽²⁾

Tumor-specific antigens (TSAs) presented on the cancer cells are used as the antigen for producing cancer vaccines, then the immune system will respond to the antigens by expressing antibodies against cancer cells. Since cancer antigens can deliver into blood circulation resulting in thrombosis or hemorrhage. Effective cancer vaccines are carefully designed to activate T-cells and eradicate cancer cells, fragments of cancer, or tumor antigens without detecting self-antigen. Cancer vaccines can use peptides, immune cells, tumor cells, or DNA as the template.

Cellular therapy⁽²⁾

Cell-based immunotherapies are the induction or modification of cells for cancer metastasis treatment. Adoptive T-cell therapy collected from the donor or the patient will be engineered and infused back into a cancer patient. Cell-based therapies have emerged as promising for improving anti-tumor activity, such as tumor-infiltrating lymphocyte, TCR-engineered T-cell, and chimeric antigen receptor T-cell (CAR T-cell).

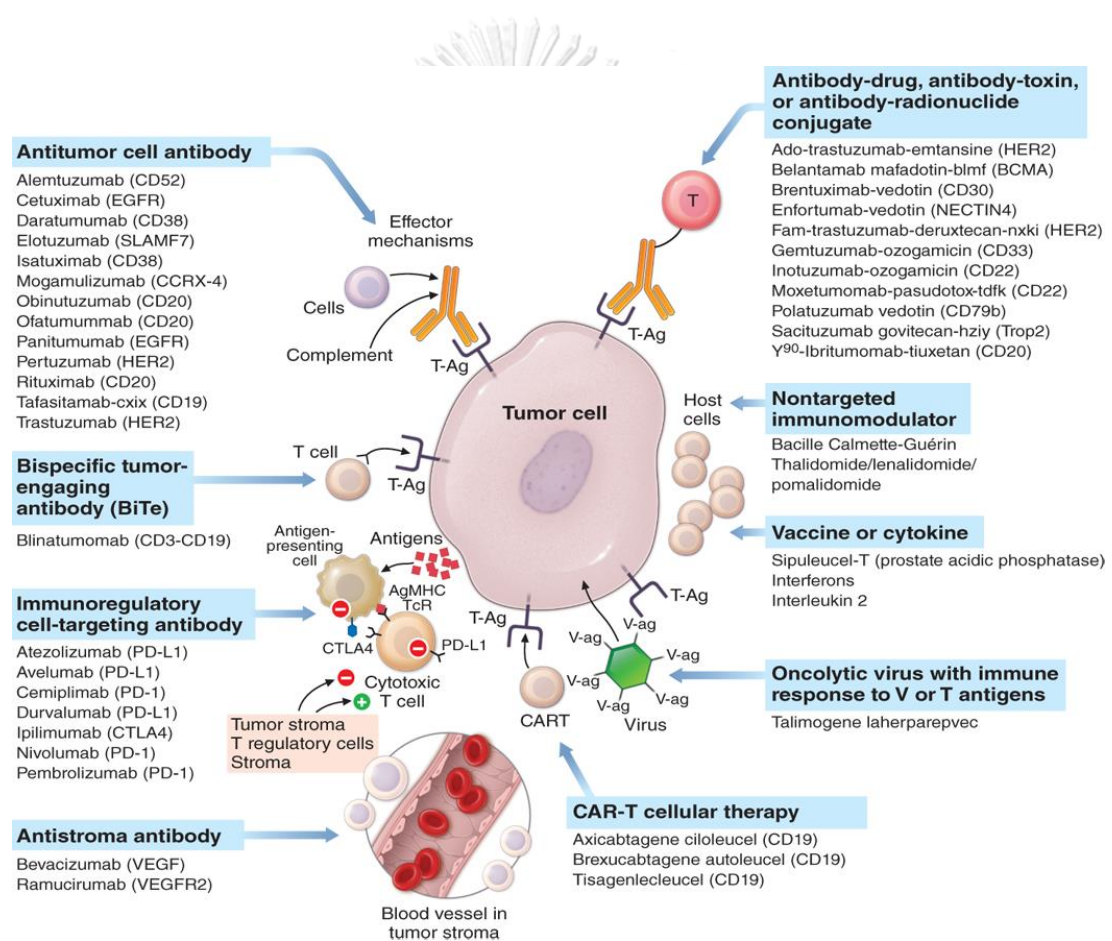


Figure 4: Cancer immunotherapy agents. ⁽³⁸⁾

2.3 Immune checkpoint

Cancers have been developed from genetic and epigenetic alterations which have expressed tumor-associated antigens on the cancer cell membrane. T-cells, which are adaptive immune cells, are regulated by binding T-cell ligands to T-cell receptors to amplify co-stimulatory or inhibitory signals. Usually, immune checkpoints are provided for controlling autoimmunity and overcoming effective anti-tumor activity. However, the immune checkpoints also are disturbed by the cancer evasion mechanisms. T-cells are interested as therapeutic targets because of their functions; they promote the innate immune system by CD4⁺ helper T cells and kill cytotoxic cells by CD8⁺ effector T cells. ^(6, 43) Thus, immune checkpoint inhibitors are proposed by focusing on T-cells.

The roles of T-cells are as follows; recognition of antigens, development to CD4⁺ or CD8⁺, migration to the sources of antigen, and mediation through immune processes. All functions are balanced on stimulatory and inhibitory regulation. While T-cell activation checkpoints are not absolutely expressed in cancers, inhibitory checkpoints are regularly overexpressed on cancerous cells. They can be soluble or membrane-bound immune checkpoints resulting in antibody development for improving anti-tumor potential with varying functions. ^(6, 43-45)

The inhibitors of immune checkpoints are approved for cancer therapy. Cytotoxic T-lymphocyte-associated antigen 4 (CTLA4) and programmed cell death protein 1 (PD1) mainly focus on mechanisms with the capability of anti-tumor activity when used as monotherapy or in combination with other cancer immunotherapies. ^{(6,}

⁴³⁻⁴⁵⁾ Many FDA-approved immune checkpoints are presented in Table 2.

Table 2: FDA-approved immune checkpoint blockers. ⁽⁴⁶⁾

Target	Agent	Mechanism of action
New immune checkpoint inhibitors and other inhibitory targets		
CTLA-4	Ipilimumab	Inhibits T-cell deactivation
PD-1	Cemiplimab	Inhibits T-cell deactivation
	Nivolumab	Inhibits T-cell deactivation
	Pembrolizumab	Inhibits T-cell deactivation
PD-L1	Atezolizumab	Inhibits T-cell deactivation
	Avelumab	Inhibits T-cell deactivation
	Durvalumab	Inhibits T-cell deactivation

2.4 PD-1/PD-L1 checkpoint

PD-1 or Programmed cell Death 1 is a receptor on immune cells that can interact with its ligands, PD-L1 or PD-L2, to suppress immune responses. Antibodies to the PD pathway are preferred for serving in the application of various cancer therapeutics. ^(9, 47) PD-1 or PD-L1 inhibitors show the potential for anti-tumor activity and increase patient survival times. ⁽⁹⁾

PD-1 (or CD279), type I transmembrane protein receptor, contains 288 amino acids. This protein is expressed on antigen-presenting cells, including T-cells, B-cells, dendritic cells, natural killer cells, and monocytes. ^(9, 48)

PD-L1 (B7-H1 or CD274) and PD-L2 (B7-DC or CD273) are members of the B7 family. PD-L1 structure is a type I transmembrane receptor with 290 amino acid lengths. The protein is also expressed on many immune cells, such as T cells, B cells, monocytes, and antigen-presenting cells. However, pro-inflammatory cytokines, including IFN- γ and IL-4, can induce the expression of PD-L1 in some cell types. ^(9, 48) In the case of PD-L2, the protein comprises 273 amino acid residues that can be found on dendritic cells, mast cells, and macrophages. ⁽⁹⁾

The PD-1/PD-L1 axis is associated with immune responses of autoimmunity, viral infection, transplant rejection, and anti-tumor immunity. The interaction of PD-1 and PD-L1 transduces the signal to manipulate immune tolerance during inflammation and autoimmune responses.^(49, 50) However, cancer can intimate the PD-1/PD-L1 pathway to evade host immunity through various processes 1) inhibiting T-cell functions and leading them to apoptosis death, 2) decreasing the expression of inflammatory cytokines (IFN- γ , IL-2, TNF- α), and 3) overexpression of inhibitory cytokines and accelerating the development of cancer metastasis.^(9, 49) Many cancer cell signaling pathways, which are presented in Figure 5, show the relationship to PD-1 and PD-L1 expression.⁽⁵⁰⁾ Therefore, antibodies targeted to PD-1 or PD-L1 can inhibit cancer escape mechanisms. Nowadays, the Food and Drug Administration (FDA) has approved three PD-1 antibodies and three anti-PD-L1, shown in Table 2. Immune checkpoint inhibitors are monoclonal antibodies produced by B-cell specific clones, which can remarkably decrease toxicity, increase anti-tumor efficacy, inhibit metastases, and improve survival rates.⁽⁴⁸⁾

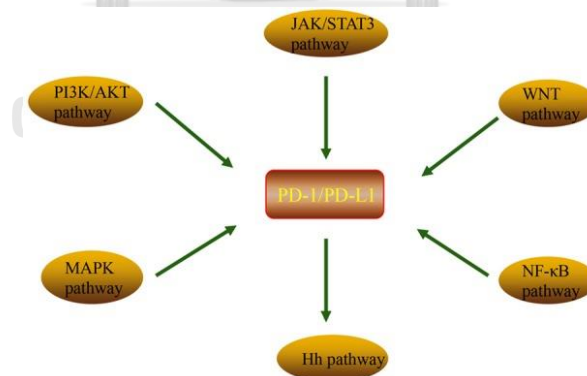


Figure 5: Signaling pathway involved with PD-1 and PD-L1 expression.⁽⁴⁸⁾

2.5 Atezolizumab

Atezolizumab, or MPDL3280A, is officially marketed under the trade name Tecentriq[®]. Atezolizumab is a non-glycosylated humanized IgG1 monoclonal antibody with a molecular weight of 145 kDa targeting programmed cell death ligand 1 to interrupt the interaction of PD-1/PD-L1. The antibody is engineered by recombinant DNA technology and then is expressed in Chinese Hamster Ovary (CHO) cells.^(9, 51, 52) The Fc region of Atezolizumab is substituted asparagine to alanine at 298 positions to minimize Fc effector function with antibody-dependent cell-mediated cytotoxicity (ADCC).⁽⁵³⁾ PD-L1 is commonly expressed on tumor cells and tumor-infiltrating lymphocytes, which leading anti-tumor inhibition. Hence, atezolizumab effectively activates T-cells and other immune responses to eliminate cancer.^(9, 51) Tecentriq[®] is commercially sold with 1200 mg/20 mL or 840 mg/14 mL of atezolizumab in a vial.⁽⁵⁴⁾

In preclinical studies, atezolizumab provides a specific binding to PD-L1 without targeting PD-L2.⁽⁵³⁾ CD8+ proliferation has increased due to mediated cytokine induction when administered with atezolizumab. Moreover, the anti-tumor activity of T-cells also improves by decreasing immunosuppressive signals when atezolizumab binds to PD-L1.^(9, 55)

Clinical results have evidenced that the using atezolizumab is effective and safe in various solid cancers and hematologic malignancies. The United States Food and Drug Administration has approved atezolizumab as follows;⁽⁵⁶⁾

1. Non-Small Cell Lung Cancer (NSCLC)

Atezolizumab is used as an adjuvant for the stage II to IIIA NSCLC treatment when tumor cells have expressed PD-L1 $\geq 1\%$

Monotherapy of atezolizumab is indicated for the first-line metastatic NSCLC treatment who have high PD-L1 expression on tumors or PD-L1 stained tumor-infiltrating T-cells cover more than 10%.

Combination therapy is provided with bevacizumab, paclitaxel, and carboplatin for metastatic non-squamous NSCLC and is dispensed with paclitaxel and carboplatin for first-line metastatic non-squamous NSCLC.

2. Small Cell Lung Cancer (SCLC)

Atezolizumab combined with carboplatin and etoposide is administered for the first-line treatment in small-cell lung cancer with extensive stage.

3. Hepatocellular Carcinoma (HCC)

Atezolizumab combined with bevacizumab is administered to treat unresectable or metastatic hepatocellular carcinoma in the patient and has not been treated with other systematic therapies.

4. Melanoma

Atezolizumab is co-administered with cobimetinib and vemurafenib in BRAF V600 mutation-positive unresectable or metastatic patients.

5. Alveolar Soft Part Sarcoma (ASPS)

Atezolizumab is also used for the treatment of patients two years of age and older with unresectable or metastatic ASPS.

Additionally, atezolizumab is also investigated under clinical trial phase I-III in advanced or metastatic solid tumors and hematological malignancies, for example, non-small and small cell lung cancer, melanoma, urothelial carcinoma, breast cancer, thymic carcinoma, gynecologic cancer, various gastrointestinal cancer, and multiple myeloma. ^(9, 52)

2.6 Antibody

Antibodies are applied in several fields. While polyclonal antibodies are famous for research and diagnostics, monoclonal antibodies are preferred in therapeutics. Polyclonal antibodies contain various antibodies which can induce immunogenicity in therapeutic uses. Monoclonal antibodies (mAbs) are developed by

hybridoma technology or phage display. The production in hybridomas, which is the fusion of cell lines of lived antibody-producing B cells and immortal myeloma cells, provides unique and specific antibodies in clinical treatments.⁽⁵⁷⁾ However, *in vitro* selection technology with the peptide expression on phage also emerged in the production of smaller antibody fragments.^(57, 58)

Immunoglobulins or antibodies are Y-shaped proteins constructed of two heavy chains and two light chains connecting with disulfide bonds. Antibodies have been divided into two domains: the variable region or antigen-binding site and the constant region interacting with effector cells and other molecules, as specified in Figure 6. There are five types of immunoglobulins classified into IgA, IgD, IgE, IgM, and IgG (defined as α , δ , ϵ , μ , and γ , respectively), characterized by constant regions. However, Immunoglobulin G (IgG) is widely applied as therapeutic antibodies because IgGs are monomers, while IgA are dimers and IgM are pentamers.^(59, 60)

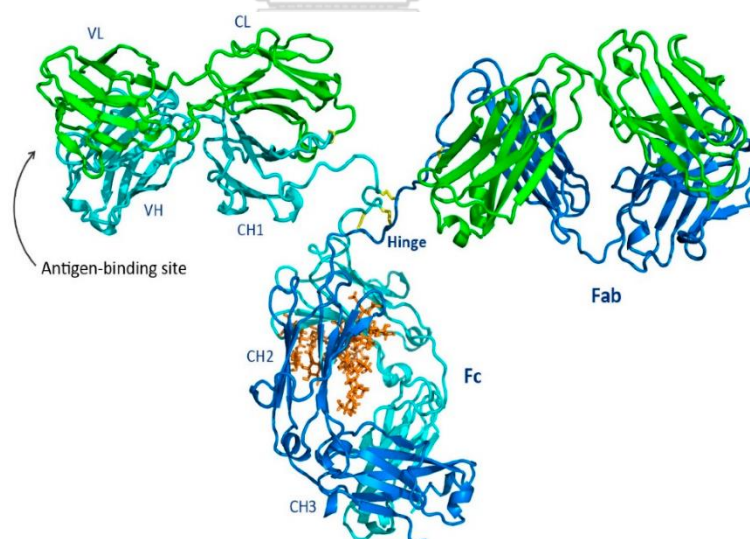


Figure 6: Antibody structure.⁽⁵⁹⁾

VL: Variable region of light chain, CL: Constant region of light chain,
VH: Variable region of heavy chain, CH: Constant region of heavy chain

IgG molecular weight is approximately 150 kDa, which comprises two heavy chains (50 kDa) and two light chains (25 kDa). IgGs can be classified into IgG1, IgG2, IgG3, and IgG4 (named $\gamma 1$, $\gamma 2$, $\gamma 3$, and $\gamma 4$, respectively), which differentiated with characteristics of four interchain and four intrachain disulfide bonds. Fragment of antigen-binding (Fab) sites (variable region) contains 110 amino acids for targeting to antigen, whereas fragment of crystallizable (Fc) sites is conserved for antibody effector functions. ^(59, 60)

Normally, IgGs are glycosylated in many sites, both N-linked glycosylation and O-linked glycosylation found in post-translational modification. However, N-linked glycosylation on the heavy chain's asparagine residue is the most interesting site because it is susceptible to immune-mediated functions. N-glycosylation residues are identified with Asn-X-Ser/Thr (X can be any amino acid except Pro), and O-linked glycosylation is specified only Ser or Thr. ⁽⁵⁹⁻⁶¹⁾

Glycosylation in the Fc region is essential for antibody effector function. Several commercial antibodies remove glycan on IgGs to inactivate the function of antibody-dependent cellular cytotoxicity (ADCC) and complement-dependent cytotoxicity (CDC). However, Fab glycosylation may decrease antigen binding specificity. ^(59, 60, 62)

The variable regions contain three complementarity-determining regions (CDRs) in each chain to create specificity of antibodies. The constant regions have three main effector functions: binding to immune cell receptors to develop ADCC, binding with complement to initiate cell lysis complex (complement-dependent cytotoxicity; CDC) or recruiting phagocytes (antibody-dependent cellular phagocytosis; ADCP), and providing antibody secretion in tears and milk. ^(59, 60, 62)

Protein glycosylation is discovered in eukaryotes, both N-linked and O-linked glycans. The core mannose complex glycans are indistinguishable between plants and mammals, but other glycosylation complexes in plants entirely differ from

mammalians. Although glycosylation variations may affect immunogenicity, there is no published evidence of immunogenicity of plant glycan in clinical trial studies.⁽⁶³⁾

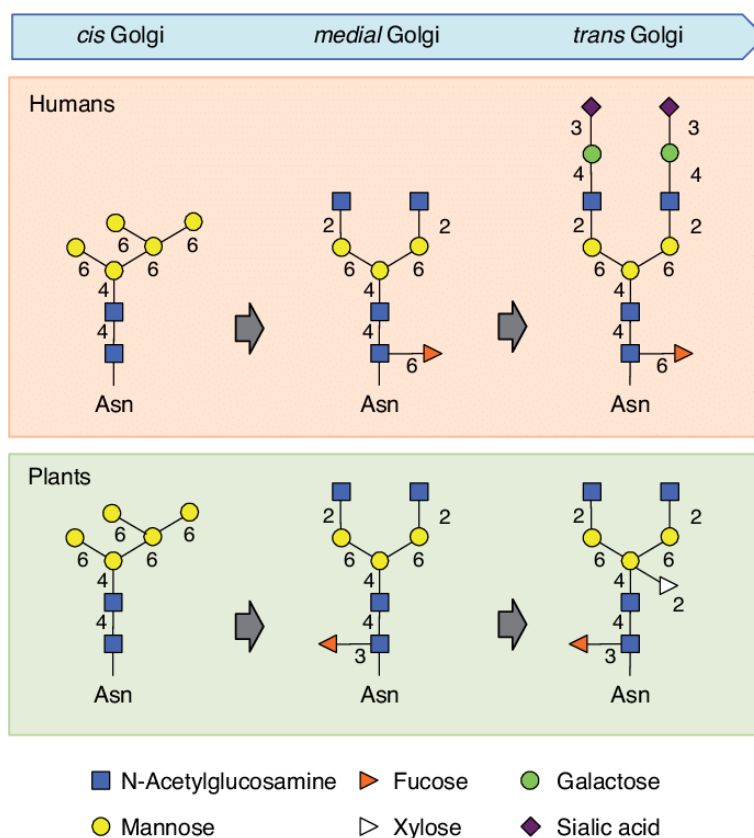


Figure 7: N-Glycosylation patterns in plants and animals.⁽⁶⁴⁾

2.7 Molecular pharming in *Nicotiana benthamiana*

Recombinant proteins are the expressed proteins in a living organism based on the knowledge of recombinant DNA technology. Therapeutic recombinant proteins have been interesting in recent decades in the pharmaceutical industry.^(65, 66) However, proteins are larger and more complex than small chemical molecules to enable specific mechanisms of action.⁽⁶⁷⁾ Production systems have been developed on various platforms, including bacteria, mammalian cells, insects, plants, and yeast.^(17, 57) Commercial therapeutic proteins are primarily cultured in Chinese Hamster

Ovary (CHO) cell lines or *Escherichia coli* cell lines. In the case of plant platform is proposed for improving cost and yield in protein production. ⁽¹⁷⁾

Table 3: Comparison of recombinant protein expression systems. ⁽¹⁷⁾

Expression system	Advantages	Disadvantages
Bacterial	<ul style="list-style-type: none"> - Ease to modification with genetic engineering - Well-understood cell lines - Simple, rapid, and scalable production - Cost-effective process - Available products approved by FDA 	<ul style="list-style-type: none"> - Non-glycosylated proteins - Not suitable for complex protein production
Insect	<ul style="list-style-type: none"> - High expression levels - Scalable production - Provide post-translational modification - Available products approved by FDA 	<ul style="list-style-type: none"> - Non-human glycosylation pattern - Unrequired post-translational modifications
Mammalian cell	<ul style="list-style-type: none"> - Provide human-like post-translational modifications - High protein yields - The most interesting and acceptable platform - Available products approved by FDA 	<ul style="list-style-type: none"> - High cost of production - Require the understanding of complex host cells - Risk of contamination with virus pathogen - Unstable cell lines - Challenging in scale-up
Plant	<ul style="list-style-type: none"> - Simple, rapid, and scalable production - Cost-effective process - Low risk of contamination with virus pathogen - Capable of complex protein modifications 	<ul style="list-style-type: none"> - Non-human glycosylation pattern - Regulatory limitations

Expression system	Advantages	Disadvantages
Yeast/ filamentous fungi	<ul style="list-style-type: none"> - Ease to modification with genetic engineering - Simple, rapid, and scalable production - Well-understood cell lines - Capable of complex protein modifications - Available products approved by FDA 	<ul style="list-style-type: none"> - Non-human glycosylation pattern

Selection of expression system is considered with protein size, protein folding, post-translational modification, safety, genetic engineering, production yield, and optimal required environments described in Table 3. ⁽¹⁷⁾ With the limitation of expression systems, there is no one suitable for all proteins. *E. coli* is properly for small protein production with high yields, while CHO cells are selected for modification of human-like proteins. The plant may improve the challenges of *E. coli* and CHO systems by being capable of scalability, low toxicity, and cost-effectiveness. ^(17, 57)

1. Therapeutic recombinant proteins produced in the plant

The plant can facilitate various abilities, including correctly folding, disulfide linkage, protein assembly, and post-translational modification resulting in the plant being used for producing vaccines, antibodies, cytokines, enzymes, growth factors, hormones, and other therapeutic proteins. ⁽¹⁷⁾ However, recombinant proteins also are produced in many plant platforms such as cells, leaves, and whole plants, which tobacco species are famously known for rapid production, easy up-scaling, and low regulatory concerns. ⁽⁶⁸⁾

Table 4: Plant-based platforms for protein production.⁽⁶⁸⁾

Platforms	Viable species	Expression time	Application	Production size	Cost	Regulatory concern
<i>In vitro</i> culture system						
Plant cell suspensions	Tobacco, carrot, rice	1-2 weeks	Biologic drugs	Depending on capacity, up to 100,000 L	Moderate	Low
Hairy roots	<i>N. tabacum</i>	2-4 weeks	Biologic drugs	Depending on capacity, up to 20,000 L	Moderate	Low
Moss	<i>Physcomitrella patens</i>	2-4 weeks	Biologic drugs	Depending on capacity, up to 500 L	Moderate	Low
Aquatic plants						
Duckweed	<i>Lemna</i> species, <i>Spirodela</i> species	3–6 weeks	Biologic drugs, enzymes	Depending on capacity, up to 10,000 L	Low	Moderate
Microalgae	<i>Chlamydomonas reinhardtii</i> , <i>Dunaliella salina</i>	2-4 weeks	Biologic drugs	Depending on capacity, up to 10,000 L	Low	Low
Whole plants						
Transgenic plants	Tobacco, Rice, corn, soybean, safflower	3–6 months	Biologic drugs, polymers, enzymes	Unrestricted	Very low	High
Transient plants	<i>N. benthamiana</i> , lettuce	2–7 days	Biologic drugs	Limited with greenhouse	Low	Low

Plant glycosylation pattern differs from mammalian cells due to N-linked glycosylation being unique with plant-specific xylose and α -1,3-fucose sugars, while β -1,4-galactose or sialic acid can be found in a mammalian modification. Hence, plants are engineered by knocking in or knocking out various genes to produce required human-like proteins, e.g., Δ XF knocking out plant can produce more human-like therapeutic proteins. However, co-infiltration of *Agrobacterium tumefaciens* harboring designed gene and glycosylation-related enzyme gene into tobacco can express glycosylation patterns miming mammalian cell lines. These engineering strategies can overcome plant-based proteins, which have gained adequate efficacy and safety profiles. ^(17, 69, 70)

N-glycan biosynthesis in plants is very similar to other eukaryotic platforms. Oligosaccharides are assembled on PP-dolichol in the cytoplasm. When $\text{Man}_5\text{GlcNAc}_2$ is formed, it will be flipped into Endoplasmic Reticulum (ER) lumen and continue glycosylation. Proteins are initially glycosylated in ER by transferring high-mannose oligosaccharides from the dolichol lipid carrier to Asn specific residue of the protein. While the glycoprotein is transported through the secretory pathway, glucose (Glc) residues will be removed to build high-mannose glycans. If the glycoproteins are not correctly folded, they will be processed by glucosyltransferase and other enzymes in the calnexin–calreticulin (CNX–CRT) cycle. Alternatively, misfolded glycoproteins will be eradicated by ER-associated degradation machinery (ERAD). Finally, corrected proteins are processed with Golgi Apparatus (GA), which generates complex glycans with xylose, fucose, and galactose. ⁽⁷¹⁾

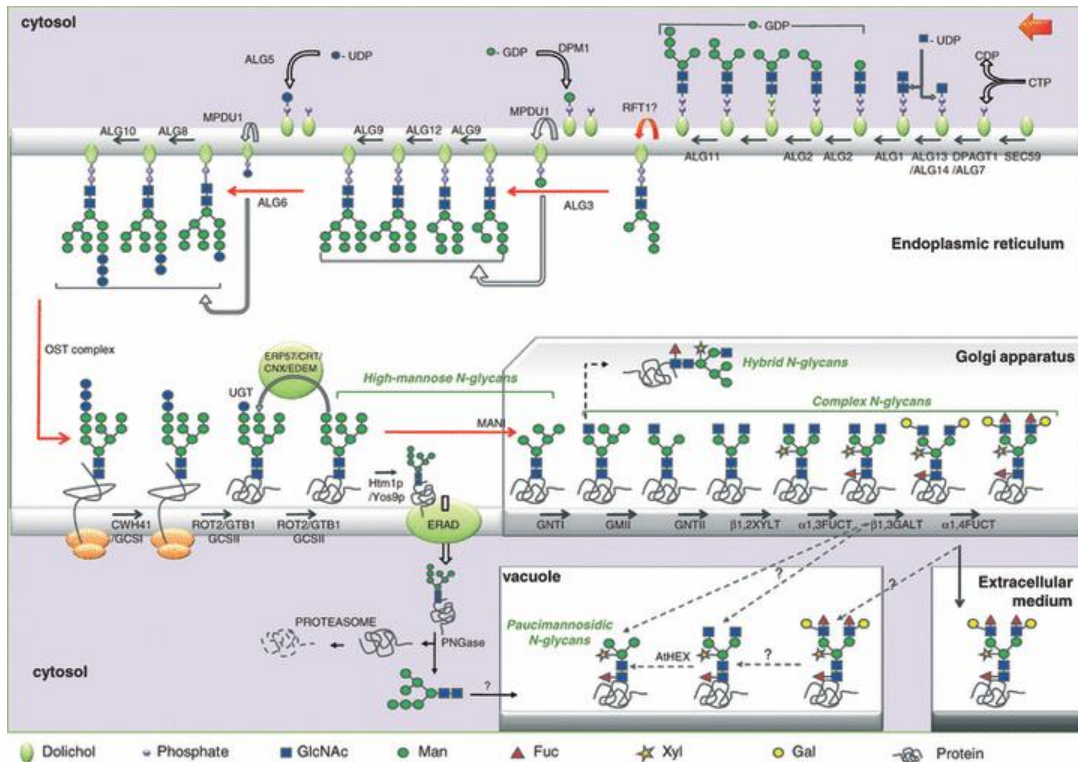


Figure 8: Schematic of protein N-glycosylation pathways in plants.⁽⁷¹⁾

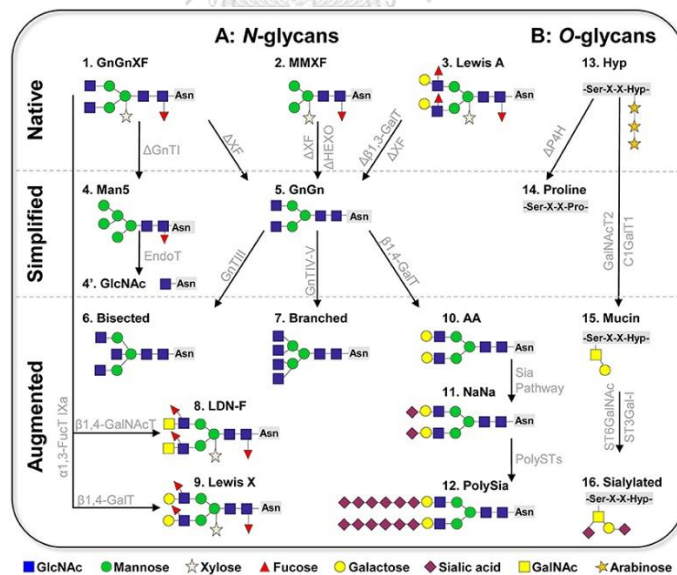


Figure 9: Schematic of plant glycosylation engineering strategies.⁽⁷⁰⁾

Native: The complex glycoforms are frequently detected in wild-type plants.

Simplified: Glycan simplification and homogeneity by knockout/down approaches.

Augmentation: Plant glycans by stable/transient overexpression of foreign glycosylation enzymes.

2. Transient expression in *Nicotiana benthamiana*

Transient expression is accomplished by the expression of *A. tumefaciens* inserting genes of interest in a recombinant expression plasmid or by viral expression vectors.^(17, 69) Recombinant proteins can be produced in a few days after infiltration of *Agrobacterium* into the leaves. Due to the high-copy plasmids being delivered to plant cells for gene transcription, transient expression maximizes the protein yields greater than stable transgenic plants. However, stable plant-expressed systems are controversial with regulatory limitations. As a result, transient expressions are interested in the investigation of biologics.⁽⁶⁸⁾

Agrobacterium is a gram-negative bacterium that causes crown gall and hairy root diseases in plants. Tumor-inducing (Ti) plasmid in *Agrobacterium tumefaciens* can induce tumor-like galls while root-inducing (Ri) plasmid in *Agrobacterium rhizogenes* can induce hairy root growth. The inducing plasmids are transferred into the plant nucleus, incorporated into host plant DNA, and then oncogenes in the T-DNA region will be translated to significant cell growth.^(33, 72, 73)

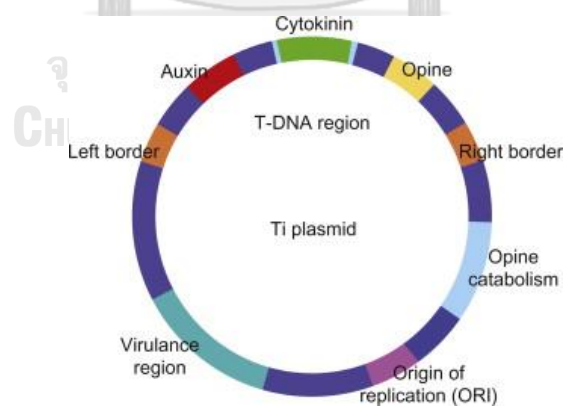


Figure 10: Structure of tumor-inducing (Ti) plasmid found in *Agrobacterium tumefaciens*.⁽⁷²⁾

The *A. tumefaciens*-mediated plant transformation process involves two essential gene regions. The first is the T-DNA border required for the incorporation gene of interest. The second is the virulence region which expresses several vir genes to transfer the gene in T-DNA into the host nucleus, as explained in Figure 10.⁽⁷³⁾

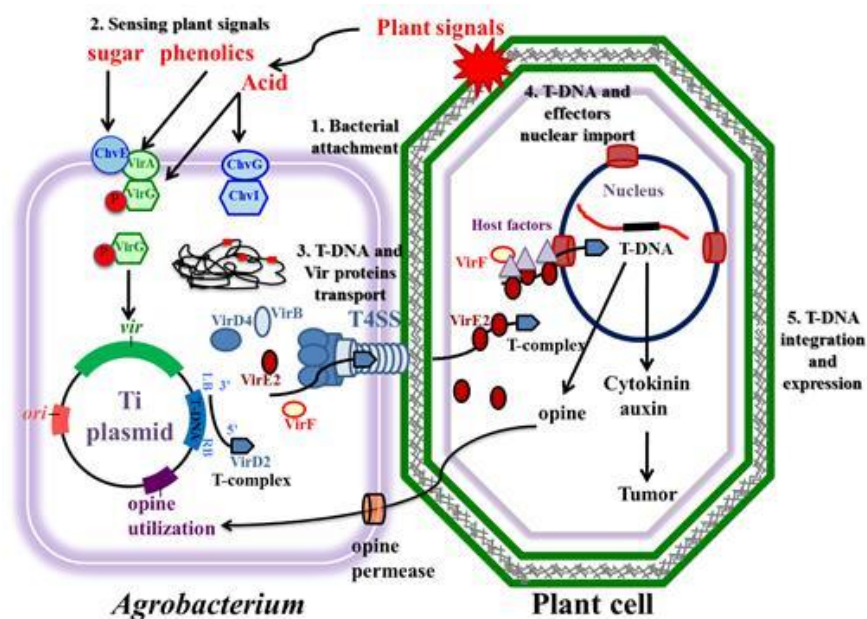


Figure 11: The essential steps of *Agrobacterium tumefaciens* transformation.⁽⁷³⁾

N. benthamiana is the most common transient expression host expression due to its ability to modify transformation processes and scale-up production. The gene of interest is introduced into plant cells by two methods.^(17, 68)

- Recombinant expression plasmids provide rapid protein expression within a few days post-infiltration, and protein yields up to 200 µg/g plant fresh weight.
- Viral mediated can express the protein in 2 weeks; however, the protein is up to 5.0 mg/g plant fresh weight.

Transient systems can also co-express with multiple genes to produce higher complex proteins, including antibodies, virus-like particles (VLP), and multichain proteins. Moreover, transient expression is easily up-scaling manufacturing

production, which can be accelerated to perform preclinical and clinical testing. Plant-based biopharmaceutical companies have complied with GMP to develop the use of agroinfiltration of *N. benthamiana*. However, harvest time also is a significant limitation of transient protein production. Finally, transient expression systems have been continuously improved for rapid, high protein yields and scalability manufacturing of recombinant proteins with the acceptance for the commercial production of various biopharmaceuticals. ^(17, 68, 69)



CHAPTER III MATERIALS AND METHODS

3.1 Materials and Equipment

3.1.1 Gene sequences

- Heavy chain of human IgG1 antibody in pGEM[®]-T Easy Vector
- Light chain of human IgG1 antibody in pGEM[®]-T Easy Vector
- Heavy chain of Atezolizumab in Blue Heron pUCminusMCS (Blue Heron Biotech, USA)
- Light chain of Atezolizumab in Blue Heron pUCminusMCS (Blue Heron Biotech, USA)

3.1.2 Plant material

- Tobacco plants (*Nicotiana benthamiana*)

3.1.3 Microorganisms

- *Escherichia coli* strain DH10B
- *Agrobacterium tumefaciens* strain GV3101

3.1.4 Cloning and expression vectors (Appendix B)

- pGEM[®]-T easy vector (Promega, USA)
- pBYR2eK2Md vector⁽⁷⁴⁾

3.1.5 Enzymes

- Restriction enzyme *Xho*I, *Xba*I, *Sac*I, *Nhe*I, *Afl*II (New England Biolabs, USA)
- Taq DNA polymerase (Vivantis, Malaysia)
- Q5[®] High-Fidelity DNA polymerase (New England Biolabs, USA)
- T4 DNA ligase and T4 DNA ligase buffer (New England BioLabs, USA)
- rCutSmart Buffer (New England BioLabs, USA)

3.1.6 Ladder

- VC 1kb DNA ladder (Vivantis, Malaysia)

- Precision Plus Protein™ Standards (Bio-Rad, USA)

3.1.7 Antibodies

- Goat anti-human IgG (Abcam, UK)
- Human IgG1 (Abcam, UK)
- Sheep Anti-Human Kappa-HRP (The Binding Site, UK)
- Sheep Anti-Human Gamma-HRP (The Binding Site, UK)
- Recombinant human PD-L1 His-tag protein (R&D Systems, USA)
- Human IgG₁ (Novus Biologicals, USA)
- HRP-conjugated goat anti-human IgG Fc-γ specific antibody (Jackson Immuno Research, USA)

3.1.8 Antibiotics (Appendix C)

- Ampicillin sodium (AppliChem, Germany)
- Gentamycin sulfate (AppliChem, Germany)
- Kanamycin sulfate (AppliChem, Germany)
- Rifampicin (TOKU-E, USA)

3.1.9 Molecular biology kits

- AccuPrep® Nano-Plus Plasmid Mini Extraction Kit (K-3111, K-3112) (Bioneer, Korea)
- AccuPrep® Gel Purification Kit (Cat.No. K-3035, K-3035-1) (Bioneer, Korea)
- Cell-based luciferase reporter assay (PD-1/PD-L1 Blockade Bioassays) (Promega, US)

3.1.10 Media (Appendix C)

- Luria-Bertani (LB) broth medium
- Luria-Bertani (LB) agar medium

3.1.11 Buffer (Appendix C)

- Infiltration buffer

- Phosphate buffered saline (PBS) buffer
- Phosphate buffered saline tween (PBST) buffer
- Running buffer
- Transfer buffer
- Z-buffer reducing condition
- Z-buffer non-reducing condition

3.1.12 Chemicals

- 1,2-Bis(dimethylamino)ethane (TEMED) (Affymetrix, USA)
- 4-Morpholineethanesulfonic acid (MES) (AppliChem, Germany)
- 5-bromo-4-chloro-3-indolyl- β -D-galactopyranoside (X-gal) (HIMEDIA, India)
- Acrylamide/Bisacrylamide 40% (HiGenoMB, India)
- Agar powder (Titan Biotech, India)
- Agarose (Vivantis, Malaysia)
- Ammonium persulfate ($((\text{NH}_4)_2\text{S}_2\text{O}_8)$, APS) (HIMEDIA, India)
- Ammonium sulfate ($(\text{NH}_4)_2\text{SO}_4$) (CARLO ERBA Reagents, Italy)
- Beta-mercaptoethanol (AppliChem, Germany)
- Bovine Serum Albumin (BSA) (HIMEDIA, India)
- Bradford reagent (Bio-Rad, USA)
- Bromophenol blue (KEMAUS, Australia)
- Color reagent A (stabilized peroxide solution) (R&D Systems, USA)
- Color reagent B (stabilized chromogen solution) (R&D Systems, USA)
- Coomassie blue R-250 (AppliChem, Germany)
- dATP, dCTP, dGTP, and dTTP (Fermentas, USA)
- Dimethyl sulfoxide (DMSO) (Merck, Germany)
- Disodium hydrogen phosphate (Na_2HPO_4) (EMSURE, Germany)
- DNA gel stain SafeGreen™ Loading Dye (Vivantis, Malaysia)

- DNA loading dye (New England Biolabs, USA)
- Enhanced Chemiluminescence (ECL) detection reagent (Abcam, UK)
- Ethanol (EMSURE, Germany)
- Ethanol, purified (Merck, Germany)
- Ethylenediaminetetraacetic acid (EDTA) (HIMEDIA, India)
- Glacial acetic acid (EMSURE, Germany)
- Glycerol (HIMEDIA, India)
- Glycine (KEMAUS, Australia)
- Heiter™ (Kao, Thailand)
- Hydrochloric acid (HCl) (Merck, Germany)
- InstantBlue™ (Expedeon, UK)
- Imidazole (AppliChem, Germany)
- Isopropyl- β -D-thiogalactopyranoside; IPTG (HIMEDIA, India)
- Magnesium sulfate (MgSO_4) (KEMAUS, Australia)
- Methanol, 95% (Chemex, Thailand)
- Miller-Luria Bertani (LB) (HIMEDIA, India)
- Nitrocellulose membrane (Bio-Rad, USA)
- Peptone (HIMEDIA, India)
- Potassium chloride (KCl) (KEMAUS, Australia)
- Potassium dihydrogen phosphate (KH_2PO_4) (CARLO ERBA Reagents, Italy)
- Sodium dodecyl sulfate (SDS) (HIMEDIA, India)
- Skim milk (Difco, USA)
- Sodium chloride (NaCl) (HIMEDIA, India)
- Sodium hydroxide (NaOH) (HIMEDIA, India)
- Sulfuric acid (H_2SO_4) (EMSURE, Germany)
- TAE buffer, 50x (Bio-Rad, USA)

- TMB stabilized substrate for horseradish peroxidase (Promega, USA)
- Tris-base (Vivantis, Malaysia)
- Tween-20 (Vivantis, Malaysia)
- Yeast extract (Titan Biotech, India)

3.1.13 Materials

- 0.45 μm sterile Filter 47 mm (Merck, Ireland)
- 1.5, 2, 5, 15, 50 mL Centrifuge tube (Axygen, USA)
- Amicon[®] Ultra 15 mL Filters 50 kDa (Merck, Ireland)
- Aquasil C18 pre-column (Thermo Scientific, USA)
- Biobasic C18 analytical column (Thermo Scientific, USA)
- Disposable cuvettes (BRAND, Germany)
- ELISA plate (Thermo Scientific, USA)
- ELISA reagent reservoir (Thermo Scientific, USA)
- Nitrocellulose membrane (Bio-Rad, USA)
- Microplate, 96 wells (Greiner Bio-One, Austria)
- MicroPulser electroporation cuvettes, 0.2 cm gap (Bio-Rad, USA)
- Millex[®] - GP 0.22 μm filter unit (Merck, Ireland)
- Parafilm[®] (Bemis, USA)
- PCR tubes/strips (Axygen, USA)
- Petri dishes plate (Hycon, Thailand)
- Pipette Tip sizes: 10, 200, 1000 μL and 5 mL (Axygen, USA)
- pH indicator strips (non-bleeding) pH 0-14 universal indicator ColorpHast[™] (Kerck KGaA, Germany)
- Protein A beads (Abcam, UK)
- Syringe 1 mL (Nipro, Thailand)
- X-ray green (MXG) film (Carestream, USA)

3.1.14 Equipment

- Blender: High-performance commercial blender BE-127A (Otto, Thailand)
- Blue light LED: Blue box (Minipcr, USA)
- SDS-PAGE and Blotting equipment (Bio-Rad, USA)
- Chemiluminescence: ImageQuant LAS4000 (GE Healthcare, USA)
- Column chromatography (Bio-Rad, USA)
- Digital balance: Mettler Toledo AG135 (Mettler Toledo, USA)
- Digital balance: Sartorius TE 1502s (Sartorius, Germany)
- Electric drill
- Electrophoresis (Bio-Rad, USA)
- Electroporation: MicroPulser™ (Bio-Rad, USA)
- Heat block: WiseThem® HB-R (Wisd laboratory instruments, Australia)
- High-speed centrifuge: Avanti (Beckman Coulter, USA)
- Hotplate stirrer: LabTech (Daihan Labtech, Indonesia)
- Incubator shaker (WiseCube, Germany)
- Incubator (Mettmert, Germany)
- Magnetic stirrer and heater (Stuart, UK)
- Microplate incubator (Hercuvan Lab Systems, UK)
- Microplate reader: SpectraMax M5 microplate reader (Molecular Devices, USA)
- Microplate reader: Cytation™ 5 cell imaging multi-mode reader (Agilent, USA)
- Mini Centrifuge (Bio-Rad, USA)
- Multichannel pipette (Cleaver scientific, UK)
- PCR machine: MJ Mini™ (Bio-Rad, USA)
- pH meter: SevenCompact™ pH meter S220 (Mettler Toledo, USA)

- MicroPipette set (Pipetman, USA)
- Power supply: PowerPac™ Basic power supply (Bio-Rad, USA)
- Refrigerator (Meling Biology&Medical, China)
- Shaker: Wiggin WS-300R (Wiggins GmbH, Germany)
- Spectrophotometer: GENESYS 30 (Thermo Scientific, USA)
- Q-TOF Ultima Global mass spectrometer (Waters, USA)
- Vacuum pump/ Vacuum chamber/ Vacuum filtration
- Vortex mixer (Vortex-2 GENIE, USA)

3.1.15 Software and database

- GeneArt™ gene synthesis software
(<https://www.thermofisher.com/order/geneartgenes/projectmgmt>)
- DrugBank (<https://go.drugbank.com/>)
- GenBank NCBI (<https://www.ncbi.nlm.nih.gov/genbank/>)
- BLAST (<https://blast.ncbi.nlm.nih.gov/Blast.cgi>)
- Clustal Omega (<https://www.ebi.ac.uk/Tools/msa/clustalo/>)
- ExPASy Bioinformatics Resource Portal
(<https://web.expasy.org/translate/>)
- New England Biolabs (<https://international.neb.com/>)

3.2 Method

3.2.1 Construction of Recombinant Vector

3.2.1.1 Gene design and gene synthesis

The amino acid sequences of Atezolizumab (Drugbank accession number: DB11595) were used for the anti-PD-L1 design shown in Figure 12. Variable regions of Atezolizumab light chain (LC) and heavy chain (HC) that were separately linked to human IgG1 kappa chain (Genbank accession number: AAA58989.1) and gamma chain (Genbank accession number: AAA02914.1) were flanked with signal peptide on the N-

terminus to enhance protein secretion and a SEKDEL (Ser-Glu-Lys-Asp-Glu-Leu) sequence on C-terminus to retain protein in ER during post-translation modification. Restrictive enzymes were ordered to facilitate molecular cloning, including XbaI, XhoI, AflII, NheI, and SacI (New England Biolabs, USA). Then, the sequences were reverse translated and codon-optimized *in silico* using GeneArt™ gene synthesis software (Thermo Scientific, USA) for the expression of the anti-PD-L1 antibody in *Nicotiana benthamiana*.

The variable regions of Atezolizumab were synthesized into Blue Heron pUCminusMCS plasmid by the BlueHeron® Biotechnology (Blue Heron Biotech, USA). The constant regions of human IgG1 were used from existing plasmids in our laboratory.

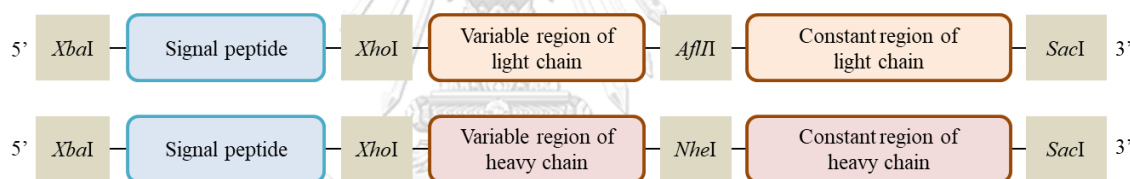


Figure 12: The schematic diagram of light chain (A) and heavy chain (B) of anti-PD-L1 for construction design.

3.2.1.2 Recombinant plasmid cloning

The variable regions preparation

The Blue Heron pUCminusMCS harboring variable regions of Atezolizumab in *Escherichia coli* strain GC10 were separately cultured in 5 mL of Luria Bertani (LB) broth medium with 100 µg/mL of Ampicillin (AppliChem, Germany) at 37 °C and 200 rpm overnight. Then, the bacterial cultures were isolated with AccuPrep® Nano-Plus Plasmid Mini Extraction Kit (K-3111, K-3112) (Bioneer, Korea). The purified vectors were individually digested with restriction enzymes and rCutSmart Buffer according to the protocol from the New England Biolabs website (New England Biolabs, USA) at 37

°C for 4 hours; additionally, *Xba*I and *Nhe*I were used for the heavy chain construct while *Xba*I and *Afl*III were used for the light chain construct. After double digestion, the products were separated with 1% w/v agarose (Vivantis, Malaysia) gel electrophoresis. The variable regions, which size around 400 bases, were cut from Blue Heron pUCminusMCS sizes 3,171 bases, then the variable regions were independently excised and purified with AccuPrep® Gel Purification Kit (Cat.No. K-3035, K-3035-1) (Bioneer, Korea).

The constant regions preparation

The pGEM®-T easy vectors (Promega, USA) harboring human IgG1 antibody were digested with *Nhe*I and *Sac*I for the heavy chain while *Afl*III and *Sac*I for the light chain. The gene products were separated by 1% w/v agarose gel electrophoresis. The constant regions show 1,006 bases for the heavy chain and 3,015 bases for the light chain. Then the gel pieces were individually cut and isolated by AccuPrep® Gel Purification Kit (Cat.No. K-3035, K-3035-1).

Expression vector preparation

Anti-PD-L1 light chain (anti-PD-L1-LC) and anti-PD-L1 heavy chain (anti-PD-L1-HC) were separately ligated into the geminiviral vector pBYR2eK2Md (pBYR2e) by double ligation protocol refer to the New England Biolabs website with *Xba*I and *Sac*I restriction enzymes. Then, the plant expression vectors were transformed into *Escherichia coli* DH10B by heat shock method. Selected colonies on LB agar with 50 µg/mL kanamycin (AppliChem, Germany) were confirmed by colony polymerase chain reaction (PCR) with the primers mentioned in Table 5 and further by sequencing. Confirmed clones were cultured in LB media with 50 µg/mL kanamycin (AppliChem, Germany) overnight at 37°C and the plasmids were isolated and transformed into *Agrobacterium tumefaciens* GV3101 strain by electroporation. Positive colonies on LB agar with 50 µg/mL of rifampicin (TOKU-E, USA), 50 µg/mL of gentamicin (AppliChem, Germany), and 50 µg/mL of kanamycin were confirmed by

colony polymerase chain reaction (PCR) and subsequently cultured for keeping in cryo-stock with 20% glycerol (HIMEDIA, Germany) at -80°C.

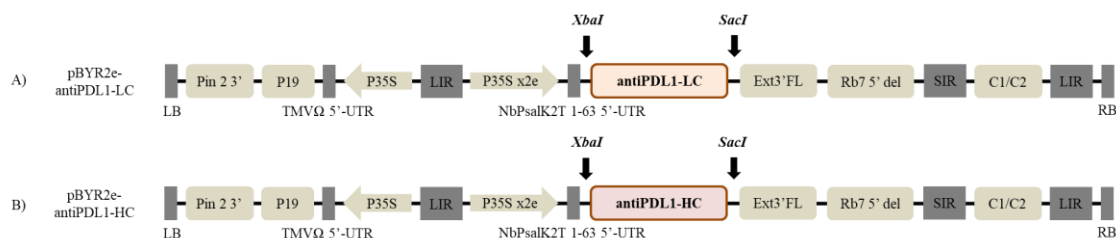


Figure 13: The schematic diagram of T-DNA regions in geminiviral vector (pBYR2e) for the plant-produced anti-PD-L1 antibody expression.

Pin 2 3': Potato proteinase inhibitor II terminator, P19: P19 silencing suppressor from Tomato Bushy Stunt Virus (TBSV), TMVΩ 5'-UTR: 5' untranslated region (UTR) of Tobacco Mosaic Virus Ω, P35S: 35S promoter from Cauliflower Mosaic Virus (CaMV), P35Sx2e: 35s promoter from Cauliflower Mosaic Virus with duplicated enhancer, NbP 5': 5' UTR of Nicotiana photosystem I reaction center subunit psa K, XbaI and SacI: restriction enzyme sites for cloning gene of interest, anti-PD-L1-LC: light chain of anti-PD-L1 gene, anti-PD-L1-HC: heavy chain of anti-PD-L1 gene, Ext3'FL: expressed sequence tags- 3' full length of tobacco extension gene, Rb7: Tobacco Rb7 promoter, C2/C1: Bean Yellow Dwarf Virus (BeYDV) ORFs C1 and C2 which encode the replication initiation protein (Rep) and RepA, LIR: long intergenic region of the BeYDV genome, SIR: short intergenic region of the BeYDV genome, LB and RB: the left and right borders of the Agrobacterium T-DNA region.

Table 5: Primers used in PCR for confirming the selected bacterial clones.

Primer	Sequence
Forward primer: <i>XbaI</i> -SP	5' TCTAGAACAAATGGGCTGG
Reverse primer: <i>SacI</i> -KD	5' CGAGCTCTCAAAGCTCATCCTTCTCAGA

3.2.2 Transient Expression with Optimization Conditions of Anti-PD-L1 Antibody in *Nicotiana benthamiana*

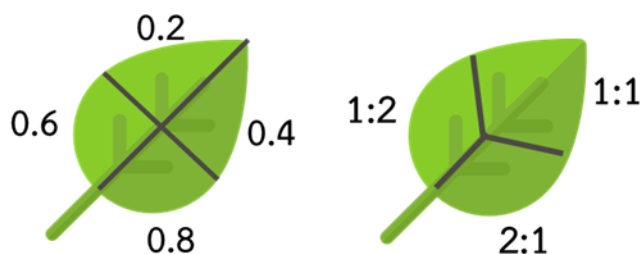


Figure 14: Pattern for agroinfiltration in optimization of antibody expression experiment which determines optimum optical density (left), day post-infiltration, and heavy chain-to-light chain ratio (right)

The cultures of *A. tumefaciens* expressing light chain and heavy chain of anti-PD-L1 antibody were grown overnight in Luria Bertani (LB) broth with 50 µg/mL of rifampicin (TOKU-E, USA), 50 µg/mL of gentamicin (AppliChem, Germany) and 50 µg/mL of kanamycin at 28°C and 200 rpm. The overnight cultures of *A. tumefaciens* harboring *pBYR2e:anti-PD-L1 LC* and *pBYR2e:anti-PD-L1 HC* were used for agroinfiltration. The *Agrobacterium* cell suspensions containing light chain and heavy chain of anti-PD-L1 were diluted with infiltration buffer (10 mM 2-(N-morpholino)-ethanesulfonic acid (MES) and 10 mM MgSO₄, pH 5.5) to get the final OD of 0.2, 0.4, 0.6 and 0.8 at 600 nm. The ratio of light chain and heavy chain used for agroinfiltration was 1:1 and each optical density (OD) concentration was co-infiltrated into the leaves of *N. benthamiana* plants, as shown in Figure 14. The infiltrated leaves were collected on days 2, 4, 6, 8, and 10 post-infiltrations to examine the expression levels of anti-PD-L1. After the analysis of optimum OD and days post infiltration (dpi), the ratio of heavy chain to light chain concentration was further varied to 1:1, 1:2, and 2:1. For optimization of antibody expression, the leaves were infiltrated with a syringe without a needle in three individual plants. Then, the

optimized conditions were used in large-scale production using a vacuum chamber to co-infiltrate anti-PD-L1 heavy and light chains.

Additionally, the *A. tumefaciens* cultures were checked for antibody expression compared to negative control (infiltration buffer) with SDS-PAGE and Western blot.

3.2.3 Purification of Plant-produced Atezolizumab

The leaves from the optimization experiments were collected and extracted in extraction buffer (5 mM Imidazole, 20 mM Tris-HCl, 50 mM NaCl, pH 7.4) by using an electric drill. The samples were centrifuged at 13,000 rpm for 15 min, and the supernatant collected was used to quantify the amount of antibody by ELISA. In large-scale production, the leaves collected were extracted using a blender. The crude extract was centrifuged at 13,000 rpm with the temperature maintained at 4°C for 45 min. The clear supernatant obtained was filtered with a sterile 0.45 µm filter and purified with protein-A affinity chromatography. Before sample loading, the column was equilibrated with PBS buffer (pH 7.4). The antibody specifically bound to protein-A beads, and then the proteins were washed with PBS buffer. The recombinant antibody was eluted with 0.1 M glycine at pH 2.5 and immediately neutralized with 1.5 M Tris-HCl (pH 8.8). Finally, the purified antibody was further subjected to dialysis, 0.22 µm filter sterilized and buffer exchanged with PBS (pH 7.4) in 50 kDa Amicon® ultra-15 centrifugal filter at 4°C, 13,000 rpm for 10 min.

3.2.4 Identification of Anti-PD-L1 Antibody with SDS-PAGE and Western Blotting

The purified anti-PD-L1 protein was analyzed by sodium dodecyl sulfate-polyacrylamide gel electrophoresis (SDS-PAGE) and western blotting with commercial Tecentriq® as a positive control. The samples were independently mixed with reducing buffer (125 mM Tris-HCl pH 6.8, 12% (w/v) SDS, 10% (v/v) glycerol, 22% (v/v)

β -mercaptoethanol, 0.001% (w/v) bromophenol blue) and non-reducing buffer (125 mM Tris-HCl pH 6.8, 12% (w/v) SDS, 10% (v/v) glycerol, 0.001% (w/v) bromophenol blue). The samples were separated on 8% SDS-PAGE and then visualized by InstantBlue™ (Expedeon, UK). The antibodies were transferred to the nitrocellulose membrane for western blot (Bio-Rad, USA). The membrane was blocked with 5% skim milk for 1 h and washed with PBST. The proteins were separately detected using sheep anti-human kappa-HRP and sheep anti-human gamma-HRP conjugated antibodies (The Binding Site, UK). The membranes were washed and developed with electrochemiluminescence (ECL) plus detection reagent (Abcam, UK), and then the signal was recorded on medical X-ray green (MXG) film (Carestream, USA).

3.2.5 Quantification of Anti-PD-L1 Antibody Amount with Sandwich ELISA

Technique

The plant-produced anti-PD-L1 antibody was quantified by sandwich enzyme-linked immunosorbent assay (ELISA). Briefly, 96-well plates (Greiner Bio-One, Austria) were coated with 50 μ L of 1:1,000 dilution of goat anti-human IgG and were incubated overnight at 4°C. Then the plates were washed and blocked with 5% skim milk in PBS for 2 h at 37°C. The samples were diluted in a range of 1:1,500 to 1:100,000 for optimization and the quantification of purified antibody. 50 μ L of diluted samples were added into each well and incubated for 2 h at 37°C, where human IgG1 (Abcam, UK) was used as control to generate the standard curve. A 1:1,000 dilution of sheep anti-human kappa-HRP (The Binding Site, UK) was added and incubated for 1 h at 37°C after washing with PBST. The plates were developed by adding 50 μ L of 3,3',5,5'-Tetramethylbenzidine (TMB) substrate (Promega, USA), followed by 1M H₂SO₄ for terminating the reaction. Finally, the plates were measured at an OD of 450 nm by using SpectraMax M5 microplate reader (Molecular Devices, USA).

3.2.6 N-Glycan Analysis

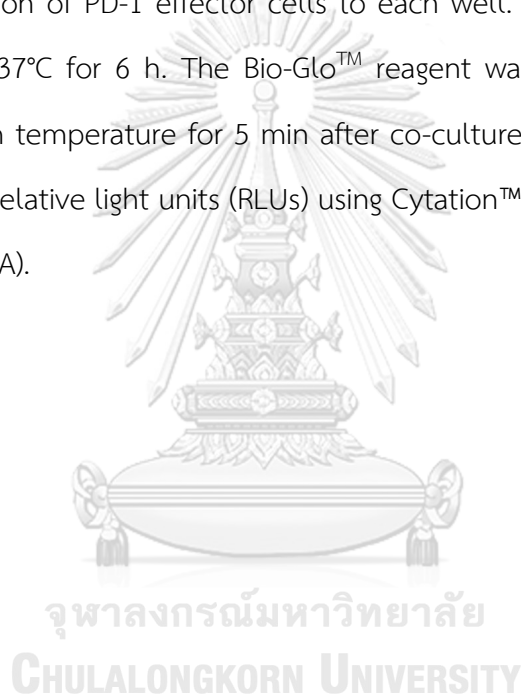
In order to evaluate the authentic glycan structures with quick and sensitive quantification, N- glycan analysis of anti-PD-L1 antibody was carried out by liquid chromatography-electrospray ionization-mass spectrometry (LC-ESI-MS) in comparison with non-glycosylated Atezolizumab. The heavy chain from purified anti-PD-L1 antibody separated on SDS-PAGE was excised from the gel, performed S-alkylation, and digested with trypsin. The peptides and glycopeptides were trapped on a 30 × 0.32 mm Aquasil C18 pre-column (Thermo Scientific, USA) and then separated on a 100 × 0.18 mm Biobasic C18 analytical column (Thermo Scientific, USA). Positive ions in the range of $m/z = 500\text{--}1600$ were monitored with a Q-TOF Ultima Global mass spectrometer (Waters, MA, USA).

3.2.7 Human PD-L1 Specific Binding Assay

The specificity of the plant-produced anti-PD-L1 antibody with human PD-L1 was evaluated by sandwich ELISA. Briefly, the MaxiSorp high protein-binding capacity 96-well ELISA plate (Thermo Scientific, USA) was coated with 100 $\mu\text{L}/\text{well}$ of recombinant human PD-L1 His-tag protein (R&D Systems, USA) at a concentration of 0.2 $\mu\text{g}/\text{mL}$, overnight at 4°C. The plate was washed three times and blocked with PBST. Two-fold serial dilutions of Tecentriq[®], plant-produced anti-PD-L1 antibody, and human IgG₁ (Novus Biologicals, USA) starting from 2 $\mu\text{g}/\text{mL}$ were added to the plate (100 $\mu\text{L}/\text{well}$) and incubated for 1 h at 37°C. Then, HRP-conjugated goat anti-human IgG Fc- γ specific antibody (Jackson Immuno Research, USA), diluted (1:10,000) in PBST (100 $\mu\text{L}/\text{well}$), was added and incubated for 1 h at 37°C. The plate was washed and developed with 100 $\mu\text{L}/\text{well}$ of SIGMAFAST™ OPD substrate solution in the dark for 20 min at room temperature. The reaction was stopped by adding 50 $\mu\text{L}/\text{well}$ of 1M H₂SO₄ and the absorbance was measured at 492 nm using a Cytation™ 5 cell imaging multi-mode reader (Agilent, USA).

3.2.8 PD-1/PD-L1 Blockade Bioassay

Following the manufacturer's instructions, the potential neutralization of PD-1/PD-L1 receptor binding with plant-produced anti-PD-L1 antibody was analyzed by cell-based luciferase reporter assay (PD-1/PD-L1 Blockade Bioassays, Promega, USA). Briefly, PD-L1 aAPC/CHO-K1 cells were seeded into a flat-clear bottom 96-well assay plate and incubated at 37°C in a 5% CO₂ incubator for 16 h. Serial dilutions of purified plant-produced anti-PD-L1 antibody and Tecentriq[®] were added to the plate, followed by addition of PD-1 effector cells to each well. The plate was kept in 5% CO₂ incubator at 37°C for 6 h. The Bio-Glo[™] reagent was added to the plate and incubated at room temperature for 5 min after co-culture. The Luminescence signal was measured as relative light units (RLUs) using Cytation[™] 5 cell imaging multi-mode reader (Agilent, USA).



CHAPTER IV RESULTS

4.1 Optimization Conditions for Anti-PD-L1 Expression

To produce the anti-PD-L1 antibody in *N. benthamiana*, variable regions of Atezolizumab gene were constructed with human IgG₁ flanked with signal peptide at N-terminal and SEKDEL sequence at C-terminal. The light chain and heavy chain genes were synthesized and codon-optimized for *N. benthamiana* before being cloned individually into the expression vector pBYR2e. After the confirmation of clones by PCR and sequencing, the recombinant plant expression vectors pBYR2e harboring the light and heavy chains of Atezolizumab were further transformed into *A. tumefaciens* GV3101. The anti-PD-L1 light chain and anti-PD-L1 heavy chain bacterial clones were cultured individually for co-infiltration into *N. benthamiana* leaves. The different parameters, such as bacterial culture OD, days post-infiltration (dpi), and heavy chain-to-light chain ratio, were investigated. The infiltrated leaves showed cell necrosis on 4 dpi, but significant necrosis was observed on 6 dpi as shown in Figure 15A. When the leaves were co-infiltrated in the ratio of 1:1, light chain to heavy chain, and culture OD of 0.4 at 600 nm, optimum expression level was obtained on day 6 post-infiltration (Figure 15B and 15C).

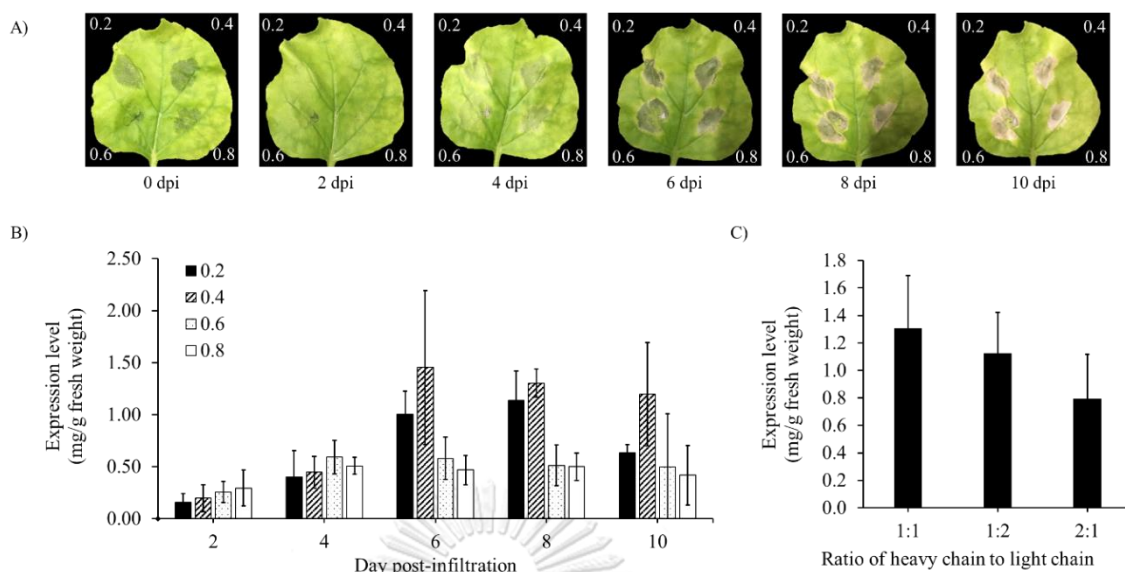


Figure 15: Optimization conditions of optical density (OD) of *Agrobacterium tumefaciens*, days post-infiltration (dpi), and heavy chain to light chain ratio.

(A) Plant-expressed anti-PD-L1 antibody at different ODs of *A. tumefaciens* on Day 0, 2, 4, 6, 8, and 10 post-infiltrations. Sandwich ELISA quantified the expression levels of anti-PD-L1 antibody. Data are represented as mean \pm SD. (B) Optimization of optical density and days post-infiltration. (C) Optimization of heavy chain to light chain ratio.

4.2 Extraction and Purification of Anti-PD-L1 from *N. benthamiana*

In the large-scale production of plant-produced anti-PD-L1, the *N. benthamiana* plants were co-infiltrated with *Agrobacterium* cultures (OD at 600 nm = 0.4) harboring the heavy chain and light chain in the ratio 1:1, respectively. The infiltrated leaves were collected after 6 dpi, extracted, and purified with protein-A affinity chromatography. The purified antibody was buffer exchanged and then analyzed by SDS-PAGE, western blotting, and sandwich ELISA. The anti-PD-L1 protein bands were observed on non-reducing SDS-PAGE at approximately 150 kDa, and the heavy chain was observed at \sim 50 kDa and the light chain at \sim 25 kDa under reducing conditions (Figure 16A). At the same time, Tecentriq[®] bands were observed at 145

kDa, 49 kDa, and 23 kDa for full antibody, heavy chain, and light chain, respectively. The anti-PD-L1 heavy and light chains were detected explicitly with sheep anti-human gamma-HRP and sheep anti-human kappa-HRP (Figure 16B and 16C). The amount of anti-PD-L1 expressed in large-scale production is 2.04 mg/mL or 86.76 µg/g fresh weight by sandwich ELISA quantification.

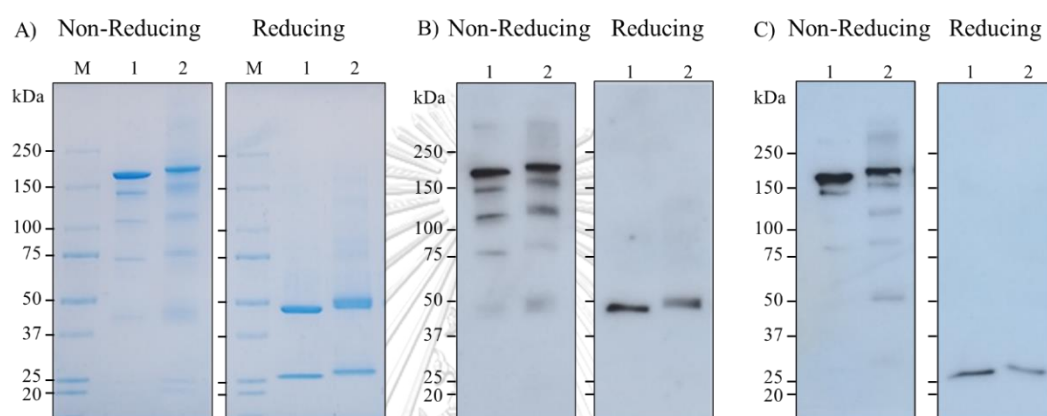


Figure 16: SDS-PAGE and Western blotting of purified anti-PD-L1 antibody under non-reducing and reducing conditions.

(A) SDS-PAGE analysis by Coomassie staining (B) Western blot analysis with sheep anti-human gamma-HRP (C) Western blot analysis with sheep anti-human kappa-HRP. kDa: Kilodalton, M: Protein marker, Lane 1: Atezolizumab (Tecentriq®) (Positive control), Lane 2: anti-PD-L1 antibody.

4.3 N-Linked Glycosylation Pattern of Anti-PD-L1 Antibody

To evaluate the N-glycan profile of plant-produced Atezolizumab, LC-ESI-MS was used. The N-glycosylation pattern of the plant-produced anti-PD-L1 antibody was compared to non-glycosylated Atezolizumab (Tecentriq®) (Figure 17), revealing that the anti-PD-L1 antibody produced in *N. benthamiana* displayed oligo-mannose glycan residues that are usually required for endoplasmic reticulum enunciated

proteins without showing any effect on the binding property of this antibody with its target.

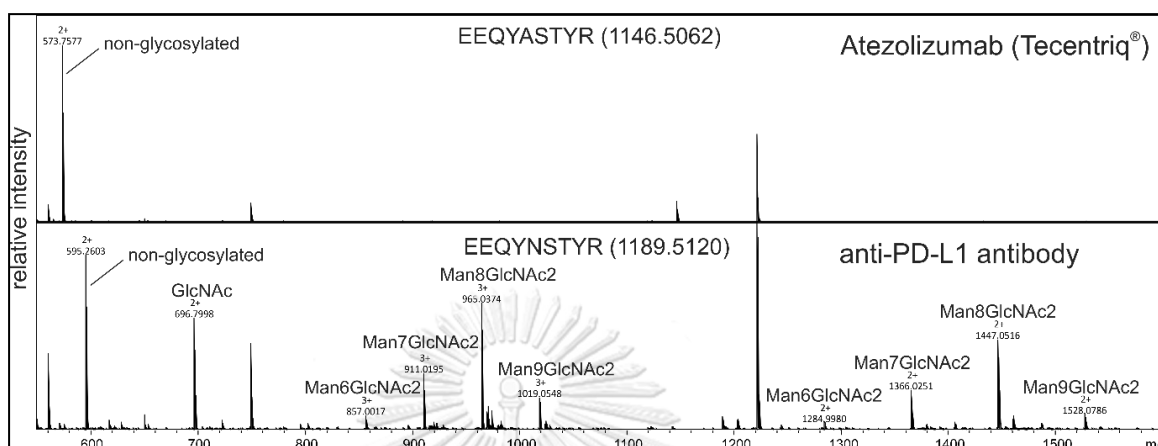


Figure 17: Liquid chromatography-electrospray ionization-mass spectrometry (LC-ESI-MS) of Tecentriq® and plant-produced PD-L1 antibody after trypsin digestion.

The N-glycosylation profile of the plant-produced glycopeptide EEQYNSTYR is depicted with other significant peaks.

4.4 Functional Assays of Plant-produced Anti-PD-L1 Antibody

The purified plant-produced anti-PD-L1 antibody binding to human PD-L1 protein *in vitro* was determined by ELISA, as shown in Figure 18A. The commercial mammalian cell-produced and plant-produced anti-PD-L1 mAbs showed similar binding to human PD-L1 protein, while the human IgG1 antibody used as negative control did not show any binding. The luciferase reporter system was used to assess the inhibitory activity of plant-produced anti-PD-L1, where serial dilutions of this antibody were added to PD-L1 aAPC/CHO-K1 cells, and the plate was incubated for 6 h. Activating luciferase expression under the control of nuclear factor of activated T-cell promoter indicates the blocking of PD-L1/PD-1 interaction in the presence of anti-PD-L1 mAb. The results indicated the inhibition of PD-L1 protein interaction with

its receptor in both plant-produced and commercial Atezolizumab with EC_{50} values of 0.0565 and 0.2195 $\mu\text{g/mL}$, respectively (Figure 18B), confirming their functionality.

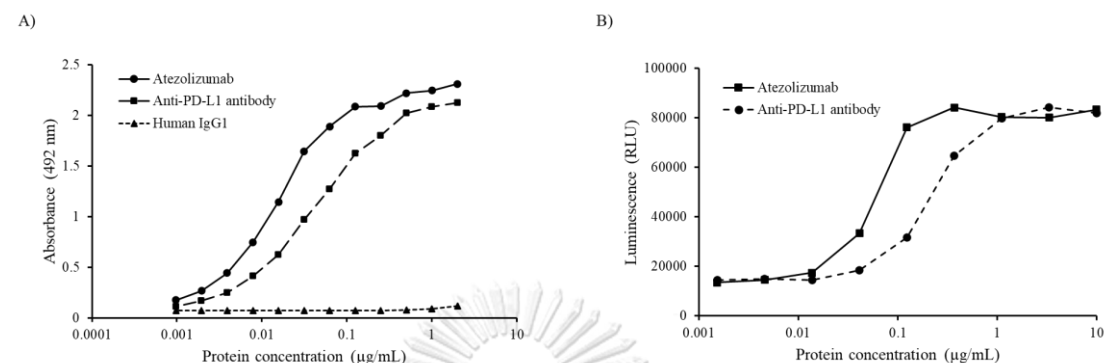


Figure 18: Binding and inhibition assays of plant-produced anti-PD-L1 antibody.

A) Specific binding to human PD-L1 by sandwich ELISA. The Tecentriq[®] and human IgG₁ were used as positive and negative control, respectively. B) PD-1/PD-L1 blockade assay for determining the inhibition activity of anti-PD-L1 antibody.

Data are represented as mean \pm SD of technical triplicates.

CHAPTER V DISCUSSION AND CONCLUSION

Immune checkpoint blockers (ICBs), as monoclonal antibodies, have gained momentum in cancer immunotherapy due to their interference in binding immune checkpoint ligands with their receptors, thereby activating T-cell immune response to eradicate cancer cells ⁽²⁾. PD-1/PD-L1 checkpoint is associated with autoimmune response of T-cells, and interestingly, PD-L1 ligands are upregulated in many tumor types, including non-small-cell lung cancer at the metastatic stage to evade the cytotoxic T-cell population, by imitating their immune responses ^(7, 42). Otherwise, they are many controversial regarding the effectiveness between the PD-1 and PD-L1 inhibitors. The PD-1 and PD-L1 inhibitors indication are investigated and approved depending on patients' characteristics, especially types of tumors, mutation, and translocation of genes (EGFR, Kras, ALK) ⁽⁷⁵⁾. Monoclonal antibodies targeting PD-L1, which the FDA approved, also overlap the epitopes, implying a structure–activity relationship of PD-1/PD-L1 blockade ⁽⁷⁶⁾. Atezolizumab is the first non-glycosylated humanized IgG1 mAb that binds explicitly to PD-L1 ligands on various types of malignant cells to eliminate the cancerous cells ⁽⁵⁴⁾. Tecentriq[®] is the official trade name of Atezolizumab which is produced in mammalian cells was approved as therapeutic for the commonly occurring metastatic non-small cell lung cancer and small cell lung cancer ⁽¹⁴⁾ involving high investment costs, verbose optimizations, sterility risks, and stringent manufacturing environments ⁽⁷⁷⁾.

In the present study, we produced anti-PD-L1 in *N. benthamiana* by cloning the Atezolizumab and human IgG1 sequences in geminiviral plant expression vector. Commercial atezolizumab is a human IgG1 without glycosylation by an N297A mutation. Deglycosylation of human IgG1 has completely removed unwanted Fc-mediated functions such as antibody-dependent cytotoxicity (ADCC). However, non-glycosylated Atezolizumab is unstable and easy to form aggregates. This study

developed glycosylated on human IgG1 of atezolizumab to improve stability without ADCC activity⁽⁷⁸⁾. The anti-PD-L1 was incorporated with signal peptide on the N-terminus to enhance protein secretion and SEKDEL sequence on C-terminus to retain the protein in ER. Due to proteins are synthesized, folded, and glycosylated in ER⁽⁷⁹⁾, the SEKDEL sequence will retain the protein in ER for necessary process. Appending SEKDEL with secretory signal peptide protein will retard protein production but enhance the amount of protein due to the secretory signal peptide lead the protein to secrete into extracellular, which reduces cytotoxicity to the cells^(80, 81).

Plant expression systems have been routinely used in recent years to produce antibodies due to ease in transformation techniques, cost-effective manufacturing, and rapid scalability⁽¹⁸⁾. The plant-produced anti-PD-L1 antibody was investigated in this study for its functional properties. As reported in previous studies, the production and expression of immune checkpoint inhibitors in *N. benthamiana* proved their efficacy in immunotherapeutics^(3, 4). Our results showed that the optimum conditions for producing the plant-produced anti-PD-L1 are bacterial density at 0.4, 6 dpi, and 1:1 of heavy chain to light chain ratio, which were used for large-scale production. The presence of high bacterial concentration leads to plant necrosis^(82, 83). Previous plant-produced protein in *N. benthamiana* studies also showed the optimum conditions during agroinfiltration. Different proteins can be expressed in different conditions of bacterial concentration, day-post infiltration, and ratio of heavy chain to light chain^(25, 27, 84, 85). However, the optimal growth of *N. benthamiana* leaves differently expressed proteins with agroinfiltration⁽⁸⁶⁾. From this study with these optimized conditions, the expression level of anti-PD-L1 mAb was found to be up to 2.04 mg/mL or 86.76 µg/g fresh weight.

The glycosylated plant-produced anti-PD-L1 bands in SDS-PAGE and Western blotting experiments were observed with higher molecular weight when compared to Tecentriq®. The plant-produced anti-PD-L1 was characterized for the chemical

entities by elucidating the N-glycosylation profile, which depicted the presence of a high number of mannose oligosaccharides (Figure 17), attributing to the target signaling in endoplasmic reticulum due to the presence of SEKDEL sequence. The structure of $\text{Man}_{5-9}\text{GlcNAc}_2$ is typically seen in N-linked glycans in plants and *N. benthamiana* ^(87, 88). SEKDEL-tagged antibodies have shown high-mannose N-glycans that are non-immunogenic ⁽⁸⁹⁾. Although previous reports show that plant-produced antibodies with mannosidic N-glycans have increased rate of antibody clearance from circulation ⁽⁹⁰⁾ and no allergic reactions or hypersensitivity responses ^(91, 92), glycan-engineered plants are an alternative to overcome these bottlenecks for use in potential therapeutic applications. However, antibody can be modified with both N-glycosylation and O-glycosylation on specific Asn sites or Ser/Thr, respectively. In order that Figure 17 can imply the pattern to other glycosylation sites.

The functional characteristics of plant-produced Atezolizumab were further assessed for binding activity and binding kinetics by ELISA and PD-1/PD-L1 blockade assay, respectively (Figure 18), confirming that this mAb effectively binds to human PD-L1 protein in similarity with Tecentriq[®] and other earlier findings ^(3, 4). By the way, the PD-1/PD-L1 blockade assay still lacks negative control to confirm their activity, but the binding assay also shows no negative control binding to PD-L1.

In conclusion, *the feasibility of N. benthamiana plant cell-based platform* was illustrated for the rapid expression of anti-PD-L1 IgG1 Atezolizumab. The present study showed similarities in PD-L1 binding efficacy and *in vitro* functional capabilities compared with mammalian cell-based antibody Tecentriq[®], thereby inferring the potentiality of plant-produced Atezolizumab for cancer therapeutics. Future studies on mammalian cells and human knock-in mice models are essential to study the *in vitro* and *in vivo* efficacy of plant-produced anti-PD-L1 Atezolizumab. Altogether, this study forms a proof of concept, paving the way to prove the reproducibility and scalability of plant expression system as an alternative platform for large-scale

manufacturing approaches, producing mAb-based checkpoint inhibitors for immunotherapy.





APPENDIX A: Amino Acid and Nucleotide Sequences

1. Amino acid sequence of the heavy chain of Atezolizumab (Drugbank accession number: DB11595)

EVQLVESGGGLVQPGGSLRLSCAASGFTFSDSWIHWRQAPGKGLEWWAWISPYGGSTYYADSVK
GRFTISADTSKNTAYLQMNSLRAEDTAVYYCARRHWPGGFDYWGQGTLLTVSSASTKGPSVFPLAP
SSKSTSGGTAALGCLVKDYFPEPVTVSWNSGALTSGVHTFPAVLQSSGLYSLSSVTVPSSSLGTQT
YICNVNHKPSNTKVDKKVEPKSCDKTHTCPPCPAPELLGGPSVFLFPPKPKDTLMISRTPEVTCWVD
VSHEDPEVKFNWYVDGVEVHNAKTKPREEQYASTYRVVSVLTVLHQDWLNGKEYKCKVSNKALPA
PIEKTISKAKGQPREPQVYTLPPSREEMTKNQVSLTCLVKGFYPSDIAVEWESNGQPENNYKTTTPVL
DSDGSFFLYSKLTVDKSRWQQGNVFCFSVMHEALHNHYTQKSLSLSPGK

2. Amino acid sequence of the light chain of Atezolizumab (Drugbank accession number: DB11595)

DIQMTQSPSSLSASVGDRVTITCRASQDVSTAWAWYQQKPGKAPKLLIYSASFLYSGVPSRFSGSGS
GTDFTLTISLQPEDFATYYCQQYLYHPATFGQGTKVEIKRTVAAPSVFIFPPSDEQLKSGTASVCL
LNNFYPREAKVQWKVDNALQSGNSQESVTEQDSKSTYLSSTLTLSKADYEKHKVYACEVTHQG
LSSPVTKSFNRGEC

3. Amino acid sequence of the constant region of human immunoglobulin gamma chain (Genbank accession number: AA02914.1)

SSASTKGPSVFPLAPSSKSTSGGTAALGCLVKDYFPEPVTVSWNSGALTSGVHTFPAVLQSSGLYSL
SSVTVPSSSLGTQTYICNVNHKPSNTKVDKKVEPKSCDKTHTCPPCPAPELLGGPSVFLFPPKPKD
TLMISRTPEVTCWVDVSHEDPEVKFNWYVDGVEVHNAKTKPREEQYNSTYRVVSVLTVLHQDWL
NGKEYKCKVSNKALPAPIEKTISKAKGQPREPQVYTLPPSRDELTKNQVSLTCLVKGFYPSDIAVEWE
SNGQPENNYKTTTPVLDSGDSFFLYSKLTVDKSRWQQGNVFCFSVMHEALHNHYTQKSLSLSPGK

4. Amino acid sequence of the constant region of human immunoglobulin kappa chain (Genbank accession number: AAA58989.1)

QLKSGTASVCLLNNFYPREAKVQWKVDNALQSGNSQESVTEQDSKDSTYLSSTLTLSKADYEKH
KVYACEVTHQGLSSPVTKSFNRGEC

5. Anti-PD-L1 heavy chain amino acid sequence (Signal peptide-Variable region of Atezolizumab heavy chain-Constant region of human gamma chain-SEKDEL)

SRTMGWSCILFLVATATGVHSDVQLLEEVQLVESGGGLVQPGGSLRLSCAASGFTFSDSWIHWVR
QAPGKGLEWVAVISPYGGSTYYADSVKGRFTISADTSKNTAYLQMNSLRAEDTAVYYCARRHWPG
GFDYWQGQGLTVTVSSASTKGPSVFPLAPSSKSTSGGTAALGCLVKDYFPEPVTVSWNSGALTSGVH
TFPAVLQSSGLYSLSSVTVPSSSLGTQTYICNVNHKPSNTKVDKKVEPKSCDKTHTCPPCPAPELL
GGPSVFLFPPKPKDTLMISRTPEVTCVVDVSHEDPEVKFNWYVDGVEVHNAKTKPREEQYNSTYR
WVSVLTVLHQDWLNGKEYKCKVSNKALPAPIEKTISKAKGQPREPQVYTLPPSRDELTKNQVSLTCL
VKGFYPSDIAVEWESNGQPENNYKTTTPVLDSDGSFFLYSKLTVDKSRWQQGNVFSCSVMHEALH
NHYTQKSLSLSPGKSEKDEL

6. Anti-PD-L1 heavy chain nucleotide sequence

TCTAGAACAAATGGGCTGGTCCTGCATCATCCTGTTCTTGCTACTGCTACCGGCGTTCACT
CTGATGTTCAACTTCTCGAGGAGGTCCAGCTCGTCGAGTCCGGCGGCGGCCTCGTCCAGCCCG
GCGGCTCCCTCCGCCTCTCCTGCGCCGCTCCGGCTTCACCTTCTCCGACTCCTGGATCCACTG
GGTCCGCCAGGCCCCCGCAAGGGCCTTGAGTGGGTCGCCTGGATCTCCCCCTACGGCGGCTC
CACCTACTACGCCGACTCCGTCAAGGGCCGCTTACCATCTCCGCCGACACCTCCAAGAACACC
GCCTACCTCCAGATGAACTCCCTCCGCGCCGAGGACACCGCCGTCTACTACTGCGCCCGCCGCC
ACTGGCCCCGGCGGCTTCGACTACTGGGGCCAGGGCACCTCGTCACCGTCTCCTCCGCTAGCA
CCAAAGGTCCATCGGTCTTTCCACTGGCACCTTCTCCAAGAGTACTTCTGGAGGCACAGCTGC
ACTGGGTTGTCTTGCAAGGACTACTTTCCAGAACCTGTTACGGTTTCGTGGAACCTCAGGTGCT
CTGACCAGTGGAGTGACACCTTTCCAGCTGTTCTTCAGTCCTCAGGATTGTATTCTCTTAGCA

GTGTTGTGACTGTTCCATCCTCAAGCTTGGGCACTCAGACCTACATCTGCAATGTGAATCACAA
 ACCCAGCAACACCAAGGTTGACAAGAAAGTTGAGCCCAAGTCTTGTGACAAGACTCATACGTGT
 CCACCGTGCCCAGCACCTGAACTTCTTGGAGGACCGTCAGTCTTCTTGTTCCTCCAAAGCCTA
 AGGATACCTTGATGATCTCCAGGACTCCTGAAGTCACATGTGTAGTTGTGGATGTGAGCCATGA
 AGATCCTGAGGTGAAGTTCAACTGGTATGTGGATGGTGTGGAAGTGCACAATGCCAAGACAAAG
 CCGAGAGAGGAACAGTACAACAGCACGTACAGGGTTGTCTCAGTTCTCACTGTTCTCCATCAAG
 ATTGGTTGAATGGCAAAGAGTACAAGTGCAAGGTCTCCAACAAAGCCCTCCCAGCCCCCATTGA
 GAAGACCATTTCCAAAGCGAAAGGGCAACCCCGTGAACCACAAGTGTACACACTTCCTCCATCT
 CGCGATGAACTGACCAAGAACCAGGTCAGCTTGACTTGCCTGGTGAAAGGCTTCTATCCCTCTG
 ACATAGCTGTAGAGTGGGAGAGCAATGGGCAACCGGAGAACAACTACAAGACTACACCTCCCGT
 TCTCGATTCTGACGGCTCCTTCTTCTCTACAGCAAGCTCACAGTGGACAAGAGCAGGTGGCAA
 CAAGGGAATGTCTTCTCATGCTCCGTGATGCATGAGGCTCTTCACAATCACTACACACAGAAGA
 GTCTCTCCTTGTCTCCGGGTAAATCTGAGAAGGATGAGCTTTGA

7. Anti-PD-L1 light chain amino acid sequence (Signal peptide-Variable region of Atezolizumab light chain-Constant region of human kappa chain-SEKDEL)

SRTMGWSCILFLVATATGVHSDVQLLEDIQMTQSPSSLSASVGDRVITICRASQDVSTAVAWYQQ
 KPGKAPKLLIYSASFLYSGVPSRFSGSGSGTDFTLTISSLQPEDFATYYCQQYLYHPATFGQGTKVEIK
 RTVAAPSVFIFPPSDEQLKSGTASVVCLLNNFYPREAKVQWKVDNALQSGNSQESVTEQDSKDSTY
 SLSSTLTLSKADYEKHKVYACEVTHQGLSSPVTKSFNRGECSEKDEL

8. Anti-PD-L1 light chain nucleotide sequence

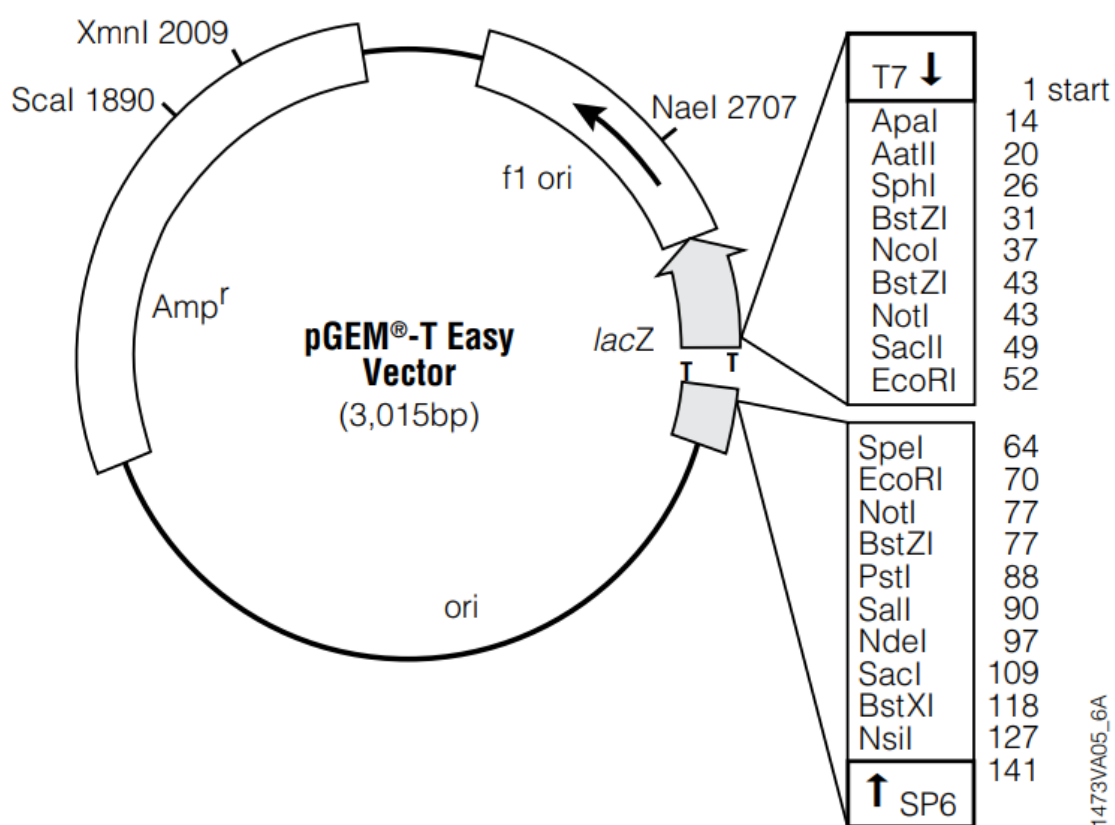
TCTAGAACAAATGGGCTGGTCCTGCATCATCCTGTTCTTGCTACTGCTACCGGCGTTCACT
 CTGATGTTCAACTTCTCGAGGACATCCAGATGACCCAGTCCCCCTCCTCCCTCTCCGCCTCCGT
 CGGCGACCGCGTCACCATCACCTGCCGCGCCTCCCAGGACGTCTCCACCGCCGTCGCCTGGTA
 CCAGCAGAAGCCCGGCAAGGCCCAAGCTCCTCATCTACTCCGCCTCCTTCTCTACTCCGGC
 GTCCCCCTCCCGCTTCTCCGGCTCCGGCTCCGGCACCGACTTCACCCTCACCATCTCCTCCCTCC

AGCCCGAGGACTTCGCCACCTACTACTGCCAGCAGTACCTCTACCACCCCGCCACCTTCGGCCA
GGGCACCAAGGTCGAGATCAAGCGCACCGTCGCCGCCCCCTCCGTCTTCATCTTCCCCCCTCC
GACGAGCAACTTAAGTCTGGAAGTCTTCTGTTGTGTGCCTTCTGAACAATTCTATCCTAGAG
AAGCCAAAGTACAGTGGAAGGTTGACAATGCTCTTCAATCAGGTAATCCCAGGAGAGTGTCAC
AGAGCAAGATTCCAAGGATTCCACCTACAGCCTCTCAAGTACCTTGACGTTGAGCAAGGCAGAC
TATGAGAAACACAAAGTGACGCATGCGAAGTCACTCATCAGGGCCTGTCATCACCCGTGACAA
AGAGCTTCAACAGGGGAGAGTGTTCTGAGAAGGATGAGCTTTGA

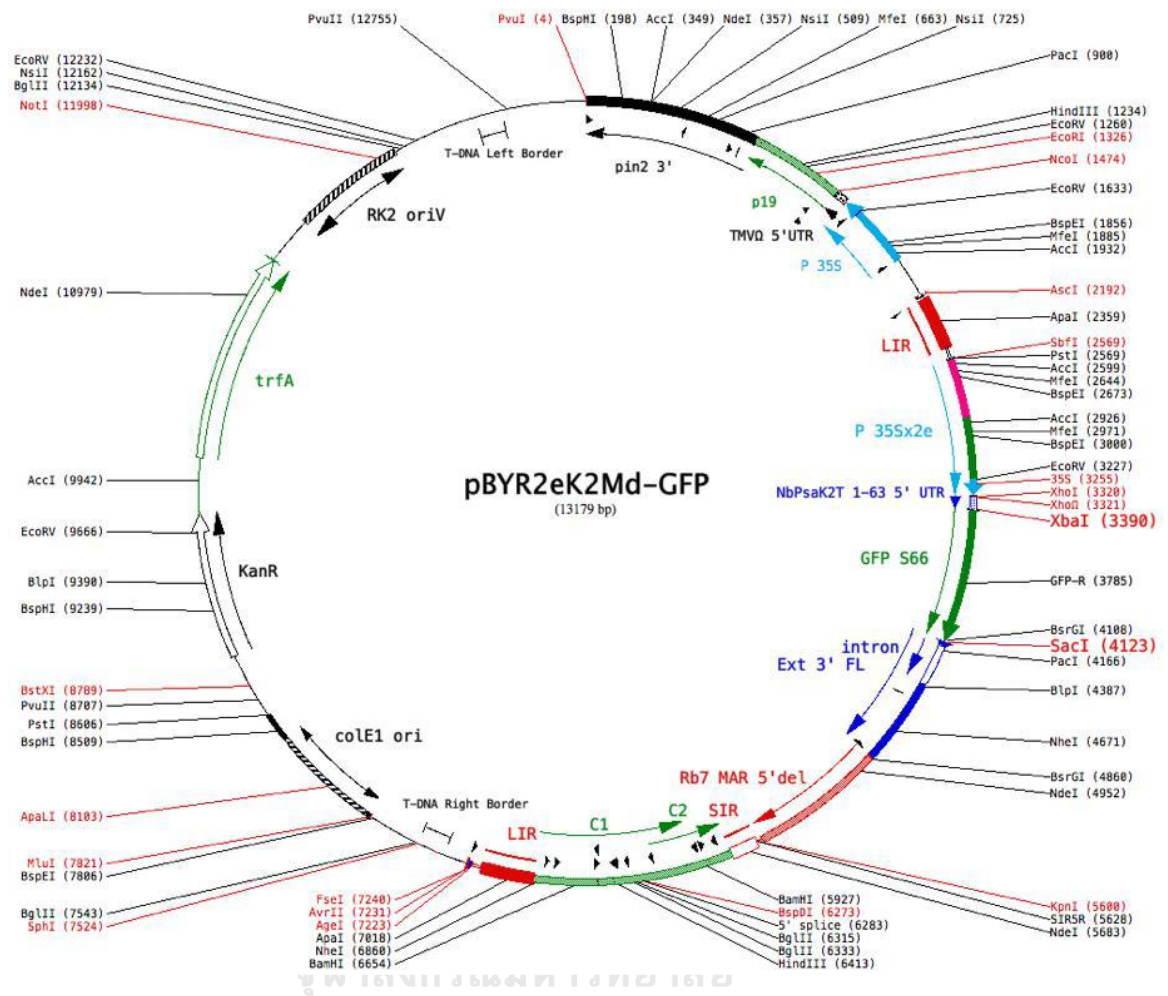


APPENDIX B: Cloning and Expression Vectors

1. pGem[®]-T easy cloning vector (Promega, USA)



2. pBYR2eK2Md geminiviral expression vector ⁽⁷⁴⁾



APPENDIX C: Chemical Solutions Preparation

1. Bacterial culture media

1.1 Luria-Bertani (LB) broth medium

Yeast extract	5	g
Peptone/Tryptone	10	g
NaCl	10	g
DI water to	1000	mL
Then autoclave		

1.2 Luria-Bertani (LB) agar medium

Yeast extract	5	g
Peptone/Tryptone	10	g
NaCl	10	g
Agar power	15	g
DI water to	1000	mL
Then autoclave		

2. Antibiotics

2.1 Ampicillin 100 mg/mL

Ampicillin	1	g
DI water to	10	mL

Filter the ampicillin solution with a 0.22 μ m filter

2.2 Rifampicin 50 mg/mL

Rifampicin	50	g
Dimethyl sulfoxide (DMSO) to	10	mL

Filter the rifampicin solution with a 0.22 μ m filter

2.3 Kanamycin 50 mg/mL

Kanamycin	50	g
DI water to	10	mL

Filter the kanamycin solution with a 0.22 μ m filter

2.4 Gentamicin 50 mg/mL

Gentamicin	50	g
DI water to	10	mL

Filter the gentamicin solution with a 0.22 μ m filter

3. Reagents

3.1 Cryostock preparation

3.1.1 50% v/v Glycerol

Glycerol	25	mL
DI water to	25	mL
Then autoclave		

3.2 Infiltration, extraction, and purification

3.2.1 10x Infiltration buffer

4-Morpholineethanesulfonic acid (MES) (pH 5.5)	21.925	g
MgSO ₄	24.648	g
DI water to	1000	mL
Then autoclave		

3.2.2 1x Infiltration buffer

10x Infiltration buffer	100	mL
DI water to	1000	mL

3.2.3 10x Phosphate buffered saline (PBS) pH 7.4

NaCl	80	g
KCl	2	g
Na ₂ HPO ₄	14.4	g

KH ₂ PO ₄	2.4	g
DI water to	800	mL
Adjust pH with 1 M NaOH to 7.4		
Adjust volume with DI water to	1000	mL
Then autoclave		
3.2.4 1x PBS pH 7.4		
10x PBS pH 7.4	100	mL
DI water to	1000	mL
3.2.5 0.05 %v/v PBS-T		
10x PBS	100	mL
Tween-20	500	μL
DI water to	1000	mL
3.2.6 1 M HCl		
Conc. HCl (12 M)	4.17	mL
DI water to	50	mL
3.2.7 0.2 M Glycine		
Glycine (MW=75.07)	15	g
DI water to	1000	mL
3.2.8 0.1 M Glycine pH 2.7		
0.2 M Glycine	100	mL
Adjust pH with 1M HCl to 2.7		
Adjust volume with DI water to	200	mL

3.3 Bradford assay

3.3.1 Bradford reagent

Bradford reagent (Bio-Rad, USA)	50	mL
DI water to	200	mL

3.4 SDS-PAGE and western blot analysis

3.4.1 10% w/v Sodium Dodecyl Sulphate (SDS) solution

SDS	10	g
Adjust volume with DI water to	10	mL

3.4.2 10% Ammonium persulfate ((NH₄)₂S₂O₈)

Ammonium persulfate	1	g
Adjust volume with DI water to	10	mL

3.4.3 1 M Tris-HCl pH 6.8

Tris-base (MW=121.14)	121.14	g
DI water to	800	mL
Adjust pH with 1M HCl to 6.8		
Adjust volume with DI water to	1000	mL

3.4.4 1.5 M Tris-HCl pH 8.8

Tris base (MW=121.14)	181.71	g
DI water to	800	mL
Adjust pH with 1M HCl to 8.8		
Adjust volume with DI water to	1000	mL

3.4.5 2 M Tris-HCl pH 7.4

Tris-base (MW=121.14)	242.28	g
DI water to	800	mL
Adjust pH with 1M HCl to 7.4		
Adjust volume with DI water to	1000	mL

3.4.6 10x Running buffer

Tris-base (MW=121.14)	30	g
Glycine (MW=75.07)	144	g
SDS (MW 288.08)	10	g
DI water to	1000	mL

3.4.7 1x Running buffer

10x Running buffer	100	mL
DI water to	1000	mL

3.4.8 20x Transfer buffer

Tris-base (MW=121.14)	30	g
Glycine (MW=75.07)	144	g
DI water to	1000	mL

3.4.9 1x Transfer buffer

20x Transfer buffer	50	mL
Methanol	150	mL
DI water to	1000	mL

3.4.10 Z-buffer reducing condition

1M Tris-HCl pH 6.8	6.25	mL
SDS	6	g
Glycerol	5	mL
Beta-mercaptoethanol	11	mL
DI water to	50	mL
0.001% w/v Bromophenol blue		

3.4.11 Z-buffer non-reducing condition

1M Tris-HCl pH 6.8	6.25	mL
SDS	6	g
Glycerol	5	mL
DI water to	50	mL
0.001% w/v Bromophenol blue		

3.4.12 Coomassie blue staining

Coomassie blue R250	1	g
Methanol	2000	mL

Glacial acetic acid	400	mL
DI water to	4000	mL=L

3.4.12 De-staining solution

Methanol	800	mL
Glacial acetic acid	400	mL
DI water to	2000	mL

3.5 ELISA analysis

3.5.1 1 M H_2SO_4

Conc. H_2SO_4 (18.4 M)	2.72	mL
DI water to	50	mL



REFERENCES

1. Zugazagoitia J, Guedes C, Ponce S, Ferrer I, Molina-Pinelo S, Paz-Ares L. Current Challenges in Cancer Treatment. *Clin Ther*. 2016;38(7):1551-66.
2. Ventola C. Cancer Immunotherapy, Part 1: Current Strategies and Agents. *P t*. 2017;42(6):375-83.
3. Phakham T, Bulaon CJI, Khorattanakulchai N, Shanmugaraj B, Buranapraditkun S, Boonkrai C, et al. Functional Characterization of Pembrolizumab Produced in *Nicotiana benthamiana* Using a Rapid Transient Expression System. *Frontiers in Plant Science*. 2021;12.
4. Rattanapisit K, Phakham T, Buranapraditkun S, Siri wattananon K, Boonkrai C, Pisitkun T, et al. Structural and In Vitro Functional Analyses of Novel Plant-Produced Anti-Human PD1 Antibody. *Sci Rep*. 2019;9(1):15205-.
5. Yiemchavee S, Wong-Arce A, Romero-Maldonado A, Shanmugaraj B, Monsivais-Urenda A, Phoolcharoen W, et al. Expression and immunogenicity assessment of a plant-made immunogen targeting the cytotoxic T-lymphocyte associated antigen-4: a possible approach for cancer immunotherapy. *Journal of Biotechnology*. 2021;329:29-37.
6. Pardoll D. The blockade of immune checkpoints in cancer immunotherapy. *Nat Rev Cancer*. 2012;12(4):252-64.
7. Topalian S, Drake C, Pardoll D. Targeting the PD-1/B7-H1(PD-L1) pathway to activate anti-tumor immunity. *Curr Opin Immunol*. 2012;24(2):207-12.
8. Liu J, Chen Z, Li Y, Zhao W, Wu J, Zhang Z. PD-1/PD-L1 Checkpoint Inhibitors in Tumor Immunotherapy. *Frontiers in Pharmacology*. 2021;12:2339.
9. Akinleye A, Rasool Z. Immune checkpoint inhibitors of PD-L1 as cancer therapeutics. *Journal of Hematology & Oncology*. 2019;12(1):92.
10. Davis AA, Patel VG. The role of PD-L1 expression as a predictive biomarker: an

analysis of all US Food and Drug Administration (FDA) approvals of immune checkpoint inhibitors. *Journal for ImmunoTherapy of Cancer*. 2019;7(1):278.

11. Deng R, Bumbaca D, Pastuskovas C, Boswell C, West D, Cowan K, et al. Preclinical pharmacokinetics, pharmacodynamics, tissue distribution, and tumor penetration of anti-PD-L1 monoclonal antibody, an immune checkpoint inhibitor. *MAbs*. 2016;8(3):593-603.
12. Dhillon S, Syed Y. Atezolizumab First-Line Combination Therapy: A Review in Metastatic Nonsquamous NSCLC. *Target Oncol*. 2019;14(6):759-68.
13. Grosser R, Cherkassky L, Chintala N, Adusumilli P. Combination Immunotherapy with CAR T Cells and Checkpoint Blockade for the Treatment of Solid Tumors. *Cancer Cell*. 2019;36(5):471-82.
14. Herbst R, Giaccone G, de Marinis F, Reinmuth N, Vergnenegre A, Barrios C, et al. Atezolizumab for First-Line Treatment of PD-L1-Selected Patients with NSCLC. *N Engl J Med*. 2020;383(14):1328-39.
15. Shah N, Kelly W, Liu S, Choquette K, Spira A. Product review on the Anti-PD-L1 antibody atezolizumab. *Hum Vaccin Immunother*. 2018;14(2):269-76.
16. Frenzel A, Hust M, Schirrmann T. Expression of recombinant antibodies. *Front Immunol*. 2013;4:217.
17. Burnett MJ, Burnett AC. Therapeutic recombinant protein production in plants: Challenges and opportunities. *PLANTS, PEOPLE, PLANET*. 2020;2(2):121-32.
18. Whaley K, Hiatt A, Zeitlin L. Emerging antibody products and Nicotiana manufacturing. *Hum Vaccin*. 2011;7(3):349-56.
19. Daniell H, Streatfield S, Wycoff K. Medical molecular farming: production of antibodies, biopharmaceuticals and edible vaccines in plants. *Trends Plant Sci*. 2001;6(5):219-26.
20. Rattanapisit K, Chao Z, Siri wattananon K, Huang Z, Phoolcharoen W. Plant-

- Produced Anti-Enterovirus 71 (EV71) Monoclonal Antibody Efficiently Protects Mice Against EV71 Infection. *Plants (Basel)*. 2019;8(12).
21. Siri wattananon K, Manopwisedjaroen S, Kanjanasirirat P, Budi Purwono P, Rattanapisit K, Shanmugaraj B, et al. Development of Plant-Produced Recombinant ACE2-Fc Fusion Protein as a Potential Therapeutic Agent Against SARS-CoV-2. *Frontiers in Plant Science*. 2021;11.
 22. Siri wattananon K, Manopwisedjaroen S, Shanmugaraj B, Rattanapisit K, Phumiamorn S, Sapsutthipas S, et al. Plant-Produced Receptor-Binding Domain of SARS-CoV-2 Elicits Potent Neutralizing Responses in Mice and Non-human Primates. *Frontiers in Plant Science*. 2021;12.
 23. Willis J, Mazarei M, Stewart C. Transgenic Plant-Produced Hydrolytic Enzymes and the Potential of Insect Gut-Derived Hydrolases for Biofuels. *Frontiers in Plant Science*. 2016;7.
 24. Xu J, Towler M, Weathers P. Platforms for Plant-Based Protein Production. *Bioprocessing of Plant In Vitro Systems*. 2018:509-48.
 25. Bulaon CJI, Shanmugaraj B, Oo Y, Rattanapisit K, Chuanasa T, Chaotham C, et al. Rapid transient expression of functional human vascular endothelial growth factor in *Nicotiana benthamiana* and characterization of its biological activity. *Biotechnology Reports*. 2020;27:e00514.
 26. Rattanapisit K, Jantimaporn A, Kaewpungsup P, Shanmugaraj B, Pavasant P, Namdee K, et al. Plant-Produced Basic Fibroblast Growth Factor (bFGF) Promotes Cell Proliferation and Collagen Production. *Planta Medica International Open*. 2020;07:e150-e7.
 27. Hanittinan O, Oo Y, Chaotham C, Rattanapisit K, Shanmugaraj B, Phoolcharoen W. Expression optimization, purification and in vitro characterization of human epidermal growth factor produced in *Nicotiana benthamiana*. *Biotechnology*

Reports. 2020;28:e00524.

28. Rattanapisit K, Yusakul G, Shanmugaraj B, Kittirotruji K, Suwatsrisakul P, Prompetchara E, et al. Plant-produced recombinant SARS-CoV-2 receptor-binding domain; an economical, scalable biomaterial source for COVID-19 diagnosis. . *Biomater Transl.* 2021;2(1):43-9.
29. Shanmugaraj B, Bulaon CJI, Malla A, Phoolcharoen W. Biotechnological Insights on the Expression and Production of Antimicrobial Peptides in Plants. *Molecules.* 2021;26(13):4032.
30. Shanmugaraj B, Khorattanakulchai N, Phoolcharoen W. Chapter 12 - SARS-CoV-2 vaccines: current trends and prospects of developing plant-derived vaccines. In: Rosales-Mendoza S, Comas-Garcia M, Gonzalez-Ortega O, editors. *Biomedical Innovations to Combat COVID-19*: Academic Press; 2022. p. 213-29.
31. Conley AJ, Zhu H, Le LC, Jevnikar AM, Lee BH, Brandle JE, et al. Recombinant protein production in a variety of *Nicotiana* hosts: a comparative analysis. *Plant Biotechnology Journal.* 2011;9(4):434-44.
32. Shanmugaraj B, Bulaon C, Phoolcharoen W. Plant Molecular Farming: A Viable Platform for Recombinant Biopharmaceutical Production. *Plants (Basel).* 2020;9(7).
33. Kapila J, De Rycke R, Van Montagu M, Angenon G. An *Agrobacterium*-mediated transient gene expression system for intact leaves. *Plant Science.* 1997;122(1):101-8.
34. Cordes LM, Shord SS. Cancer Treatment and Chemotherapy. In: DiPiro JT, Yee GC, Posey LM, Haines ST, Nolin TD, Ellingrod V, editors. *Pharmacotherapy: A Pathophysiologic Approach*, 11e. New York, NY: McGraw-Hill Education; 2020.
35. Hanahan D, Weinberg R. The hallmarks of cancer. *Cell.* 2000;100(1):57-70.
36. Sung H, Ferlay J, Siegel R, Laversanne M, Soerjomataram I, Jemal A, et al. Global Cancer Statistics 2020: GLOBOCAN Estimates of Incidence and Mortality

- Worldwide for 36 Cancers in 185 Countries. *CA: A Cancer Journal for Clinicians*. 2021;71(3):209-49.
37. Balis FM. The Goal of Cancer Treatment. *The Oncologist*. 1998;3(4):0--v.
 38. Sausville EA, Longo DL. Principles of Cancer Treatment. In: Loscalzo J, Fauci A, Kasper D, Hauser S, Longo D, Jameson JL, editors. *Harrison's Principles of Internal Medicine* 21e. New York, NY: McGraw-Hill Education; 2022.
 39. Love RR, Leventhal H, Easterling DV, Nerenz DR. Side effects and emotional distress during cancer chemotherapy. *Cancer*. 1989;63(3):604-12.
 40. Schirmacher V. From chemotherapy to biological therapy: A review of novel concepts to reduce the side effects of systemic cancer treatment (Review). *Int J Oncol*. 2019;54(2):407-19.
 41. Mellman I, Coukos G, Dranoff G. Cancer immunotherapy comes of age. *Nature*. 2011;480(7378):480-9.
 42. Raimondi C, Carpino G, Nicolazzo C, Gradilone A, Gianni W, Gelibter A, et al. PD-L1 and epithelial-mesenchymal transition in circulating tumor cells from non-small cell lung cancer patients: A molecular shield to evade immune system? *Oncoimmunology*. 2017;6(12):e1315488.
 43. Wei S, Duffy C, Allison J. Fundamental Mechanisms of Immune Checkpoint Blockade Therapy. *Cancer Discovery*. 2018;8(9):1069-86.
 44. Postow M, Callahan M, Wolchok J. Immune Checkpoint Blockade in Cancer Therapy. *J Clin Oncol*. 2015;33(17):1974-82.
 45. Topalian S, Drake C, Pardoll D. Immune Checkpoint Blockade: A Common Denominator Approach to Cancer Therapy. *Cancer Cell*. 2015;27(4):450-61.
 46. Marin-Acevedo JA, Kimbrough EO, Lou Y. Next generation of immune checkpoint inhibitors and beyond. *Journal of Hematology & Oncology*. 2021;14(1):45.
 47. Chen L, Han X. Anti-PD-1/PD-L1 therapy of human cancer: past, present, and

- future. *The Journal of Clinical Investigation*. 2015;125(9):3384-91.
48. Liu J, Chen Z, Li Y, Zhao W, Wu J, Zhang Z. PD-1/PD-L1 Checkpoint Inhibitors in Tumor Immunotherapy. *Front Pharmacol*. 2021;12:731798-.
 49. Jiang Y, Chen M, Nie H, Yuan Y. PD-1 and PD-L1 in cancer immunotherapy: clinical implications and future considerations. *Human vaccines & immunotherapeutics*. 2019;15(5):1111-22.
 50. Han Y, Liu D, Li L. PD-1/PD-L1 pathway: current researches in cancer. *Am J Cancer Res*. 2020;10(3):727-42.
 51. Shah NJ, Kelly WJ, Liu SV, Choquette K, Spira A. Product review on the Anti-PD-L1 antibody atezolizumab. *Hum Vaccin Immunother*. 2018;14(2):269-76.
 52. Markham A. Atezolizumab: First Global Approval. *Drugs*. 2016;76(12):1227-32.
 53. EMA. Assessment Report of Tecentriq. 2018.
 54. TECENTRIQ Prescribing Information. Genentech, Inc.
 55. Deng R, Bumbaca D, Pastuskovas CV, Boswell CA, West D, Cowan KJ, et al. Preclinical pharmacokinetics, pharmacodynamics, tissue distribution, and tumor penetration of anti-PD-L1 monoclonal antibody, an immune checkpoint inhibitor. *MAbs*. 2016;8(3):593-603.
 56. Inc G. Prescribing information for Tecentriq™ (atezolizumab) injection, for intravenous use. 2022.
 57. Frenzel A, Hust M, Schirrmann T. Expression of Recombinant Antibodies. *Frontiers in Immunology*. 2013;4.
 58. Hoogenboom HR. Selecting and screening recombinant antibody libraries. *Nature Biotechnology*. 2005;23(9):1105-16.
 59. Chiu ML, Goulet DR, Teplyakov A, Gilliland GL. Antibody Structure and Function: The Basis for Engineering Therapeutics. *Antibodies*. 2019;8(4).
 60. Wang W, Singh S, Zeng D, King K, Nema S. Antibody Structure, Instability, and

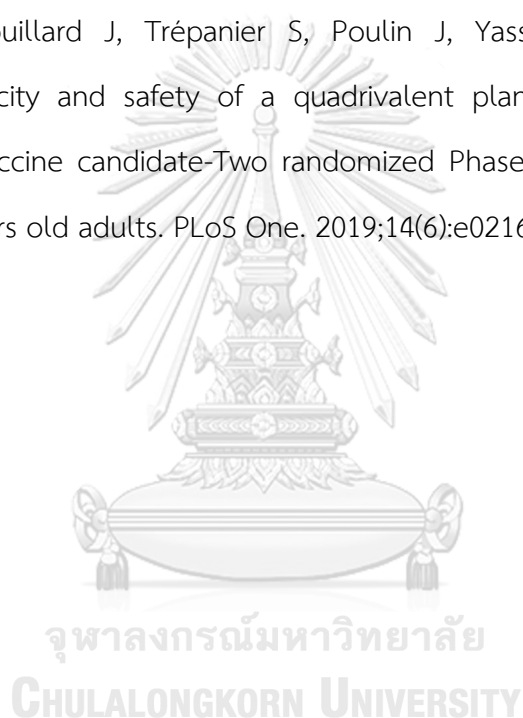
Formulation. *Journal of Pharmaceutical Sciences*. 2007;96(1):1-26.

61. Gooley AA, Classon BJ, Marschalek R, Williams KL. Glycosylation sites identified by detection of glycosylated amino acids released from Edman degradation: The identification of Xaa-Pro-Xaa-Xaa as a motif for Thr-O-glycosylation. *Biochemical and Biophysical Research Communications*. 1991;178(3):1194-201.
62. Jefferis R. Glycosylation of Recombinant Antibody Therapeutics. *Biotechnology Progress*. 2005;21(1):11-6.
63. Ma JK, Drake PM, Chargelegue D, Obregon P, Prada A. Antibody processing and engineering in plants, and new strategies for vaccine production. *Vaccine*. 2005;23(15):1814-8.
64. Orzáez D, Granell A, Blázquez M. Manufacturing antibodies in the plant cell. *Biotechnol J*. 2009;4(12):1712-24.
65. Khan S, Ullah MW, Siddique R, Nabi G, Manan S, Yousaf M, et al. Role of Recombinant DNA Technology to Improve Life. *International Journal of Genomics*. 2016;2016:2405954.
66. Andersen DC, Krummen L. Recombinant protein expression for therapeutic applications. *Current Opinion in Biotechnology*. 2002;13(2):117-23.
67. Thomas B, Van Deynze A, Bradford K. Production of therapeutic proteins in plants: UCANR Publications; 2002.
68. Xu J, Towler M, Weathers P. Platforms for Plant-Based Protein Production. In: Pavlov A, Bley T, editors. *Bioprocessing of Plant In Vitro Systems*. Cham: Springer International Publishing; 2016. p. 1-40.
69. Whaley KJ, Hiatt A, Zeitlin L. Emerging antibody products and Nicotiana manufacturing. *Hum Vaccin*. 2011;7(3):349-56.
70. Montero-Morales L, Steinkellner H. Advanced Plant-Based Glycan Engineering. *Frontiers in Bioengineering and Biotechnology*. 2018;6.

71. Gomord V, Fitchette A-C, Menu-Bouaouiche L, Saint-Jore-Dupas C, Plasson C, Michaud D, et al. Plant-specific glycosylation patterns in the context of therapeutic protein production. *Plant Biotechnology Journal*. 2010;8(5):564-87.
72. Tzotzos G, Head G, Hull R. Chapter 2 - Principles of Risk Assessment. In: Tzotzos GT, Head GP, Hull R, editors. *Genetically Modified Plants*. San Diego: Academic Press; 2009. p. 33-63.
73. Hau-Hsuan H, Manda Y, Erh-Min L. *Agrobacterium-Mediated Plant Transformation: Biology and Applications*. The Arabidopsis Book. 2017;2017(15).
74. Diamos AG, Mason HS. Modifying the Replication of Geminiviral Vectors Reduces Cell Death and Enhances Expression of Biopharmaceutical Proteins in *Nicotiana benthamiana* Leaves. *Frontiers in Plant Science*. 2019;9.
75. Alsaab HO, Sau S, Alzhrani R, Tatiparti K, Bhise K, Kashaw SK, et al. PD-1 and PD-L1 Checkpoint Signaling Inhibition for Cancer Immunotherapy: Mechanism, Combinations, and Clinical Outcome. *Frontiers in Pharmacology*. 2017;8.
76. Lee HT, Lee JY, Lim H, Lee SH, Moon YJ, Pyo HJ, et al. Molecular mechanism of PD-1/PD-L1 blockade via anti-PD-L1 antibodies atezolizumab and durvalumab. *Sci Rep*. 2017;7(1):5532.
77. Schillberg S, Raven N, Spiegel H, Rasche S, Buntru M. Critical Analysis of the Commercial Potential of Plants for the Production of Recombinant Proteins. *Frontiers in Plant Science*. 2019;10.
78. Li M, Zhao R, Chen J, Tian W, Xia C, Liu X, et al. Next generation of anti-PD-L1 Atezolizumab with enhanced anti-tumor efficacy in vivo. *Sci Rep*. 2021;11(1):5774.
79. Schwarz D, Blower M. The endoplasmic reticulum: structure, function and response to cellular signaling. *Cell Mol Life Sci*. 2016;73(1):79-94.
80. Persic L, Righi M, Roberts A, Hoogenboom HR, Cattaneo A, Bradbury A. Targeting vectors for intracellular immunisation. *Gene*. 1997;187(1):1-8.

81. Zagouras P, Rose J. Carboxy-terminal SEKDEL sequences retard but do not retain two secretory proteins in the endoplasmic reticulum. *J Cell Biol.* 1989;109(6 Pt 1):2633-40.
82. Mondal T, Bhattacharya A, Ahuja P, Chand P. Transgenic tea [*Camellia sinensis* (L.) O. Kuntze cv. Kangra Jat] plants obtained by *Agrobacterium*-mediated transformation of somatic embryos. *Plant Cell Reports.* 2001;20(8):712-20.
83. Norkunas K, Harding R, Dale J, Dugdale B. Improving agroinfiltration-based transient gene expression in *Nicotiana benthamiana*. *Plant Methods.* 2018;14:71.
84. Boonyayothin W, Sinnung S, Shanmugaraj B, Abe Y, Strasser R, Pavasant P, et al. Expression and Functional Evaluation of Recombinant Anti-receptor Activator of Nuclear Factor Kappa-B Ligand Monoclonal Antibody Produced in *Nicotiana benthamiana*. *Frontiers in Plant Science.* 2021;12.
85. Schlatter S, Stansfield SH, Dinnis DM, Racher AJ, Birch JR, James DC. On the Optimal Ratio of Heavy to Light Chain Genes for Efficient Recombinant Antibody Production by CHO Cells. *Biotechnology Progress.* 2005;21(1):122-33.
86. Ma L, Lukasik E, Gawehns F, Takken F. The Use of Agroinfiltration for Transient Expression of Plant Resistance and Fungal Effector Proteins in *Nicotiana benthamiana* Leaves. *Methods in molecular biology* (Clifton, NJ). 2012;835:61-74.
87. Rayon C, Lerouge P, Faye L. The protein N-glycosylation in plants. *Journal of Experimental Botany.* 1998;49.
88. Strasser R, Stadlmann J, Schähs M, Stiegler G, Quendler H, Mach L, et al. Generation of glyco-engineered *Nicotiana benthamiana* for the production of monoclonal antibodies with a homogeneous human-like N-glycan structure. *Plant Biotechnology Journal.* 2008;6(4):392-402.
89. Sriraman R, Bardor M, Sack M, Vaquero C, Faye L, Fischer R, et al. Recombinant anti-hCG antibodies retained in the endoplasmic reticulum of transformed plants

- lack core-xylose and core- α (1,3)-fucose residues. *Plant Biotechnol J.* 2004;2(4):279-87.
90. Reusch D, Tejada M. Fc glycans of therapeutic antibodies as critical quality attributes. *Glycobiology.* 2015;25(12):1325-34.
91. Ma J, Drossard J, Lewis D, Altmann F, Boyle J, Christou P, et al. Regulatory approval and a first-in-human phase I clinical trial of a monoclonal antibody produced in transgenic tobacco plants. *Plant Biotechnol J.* 2015;13(8):1106-20.
92. Pillet S, Couillard J, Trépanier S, Poulin J, Yassine-Diab B, Guy B, et al. Immunogenicity and safety of a quadrivalent plant-derived virus like particle influenza vaccine candidate-Two randomized Phase II clinical trials in 18 to 49 and ≥ 50 years old adults. *PLoS One.* 2019;14(6):e0216533.





จุฬาลงกรณ์มหาวิทยาลัย
CHULALONGKORN UNIVERSITY

VITA

NAME	Thareeya Phetphoung
DATE OF BIRTH	21 October 1995
PLACE OF BIRTH	Chainat, Thailand
INSTITUTIONS ATTENDED	2008-2014: Satri Nakhon Sawan School, Nakhon Sawan, Thailand 2015-2021: Doctor of Pharmacy (B. Pharm), Pharmaceutical Sciences, Chulalongkorn University, Bangkok, Thailand
HOME ADDRESS	House No. 53/7, Moo. 3, Khung Samphao Sub-district, Manorom District, Chai Nat Province, 17110, Thailand
PUBLICATION	Phetphoung T, Malla A, Rattanapisit K, Pisuttinusart N, Damrongyot N, Joyjamras K, et al. Expression of plant-produced anti-PD-L1 antibody with anoikis sensitizing activity in human lung cancer cells via., suppression on epithelial-mesenchymal transition. PLoS ONE. 2022;17(11): e0274737.